Chemical Probes for Bioimaging

Part 3: RNA AND DNA IMAGING

Kai Johnsson

Department of Chemical Biology
Max Planck Institute for Medical Research, Heidelberg

Institute of Chemical Sciences and Engineering
EPFL, Lausanne

Single-stranded RNA and DNA can fold into defined three-dimensional structures that can bind molecules and catalyze reactions

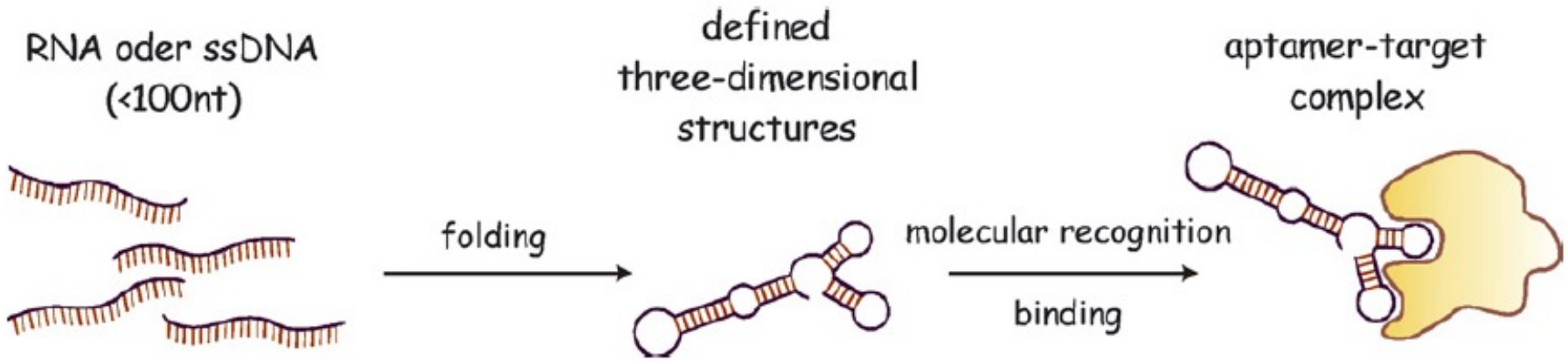

http://www.annualreviews.org/doi/pdf/10.1146/annurev.biochem.68.1.611

SELEX: *Systematic Evolution of Ligands by EXponential Enrichment*

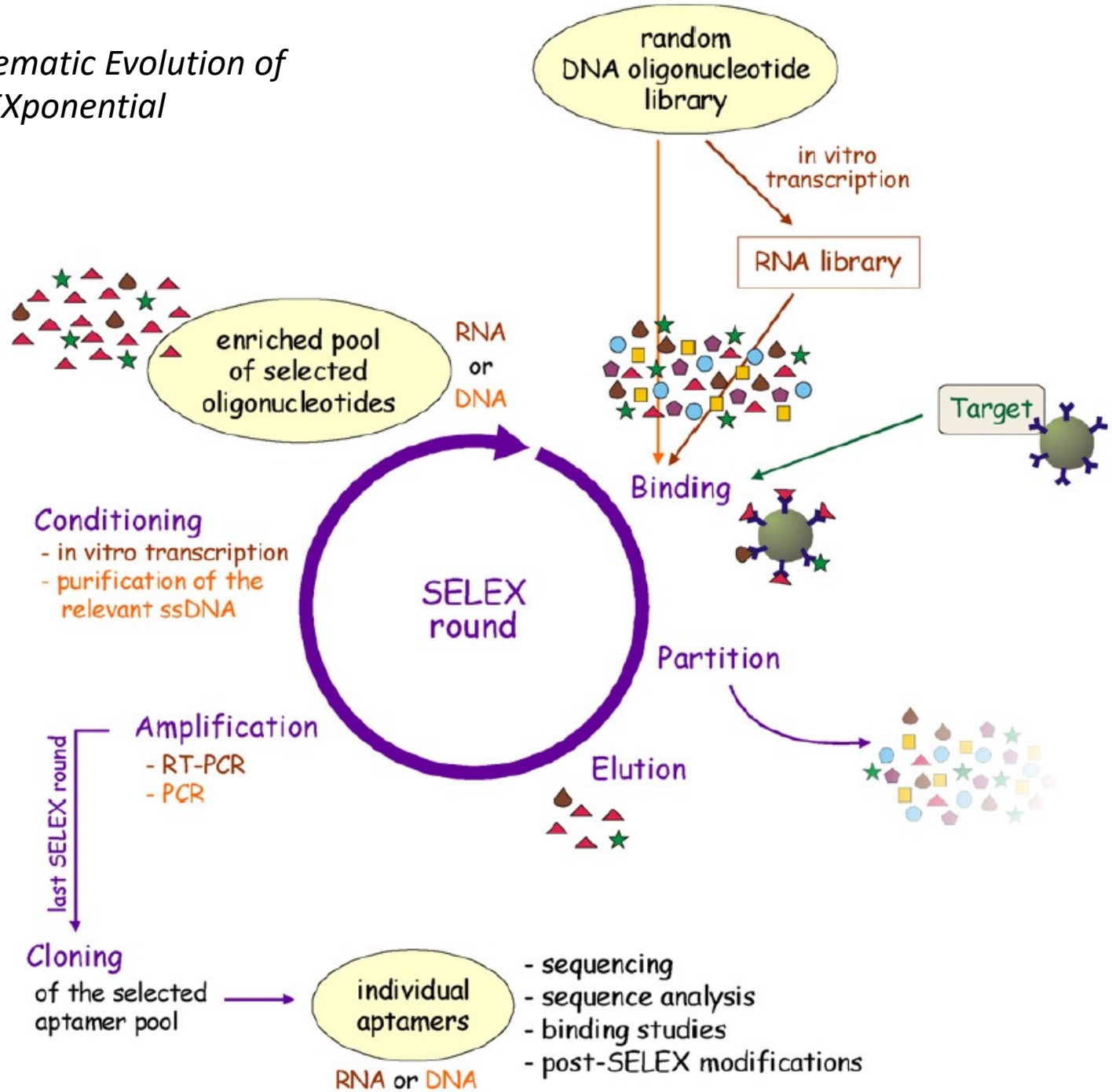

How to make RNA libraries

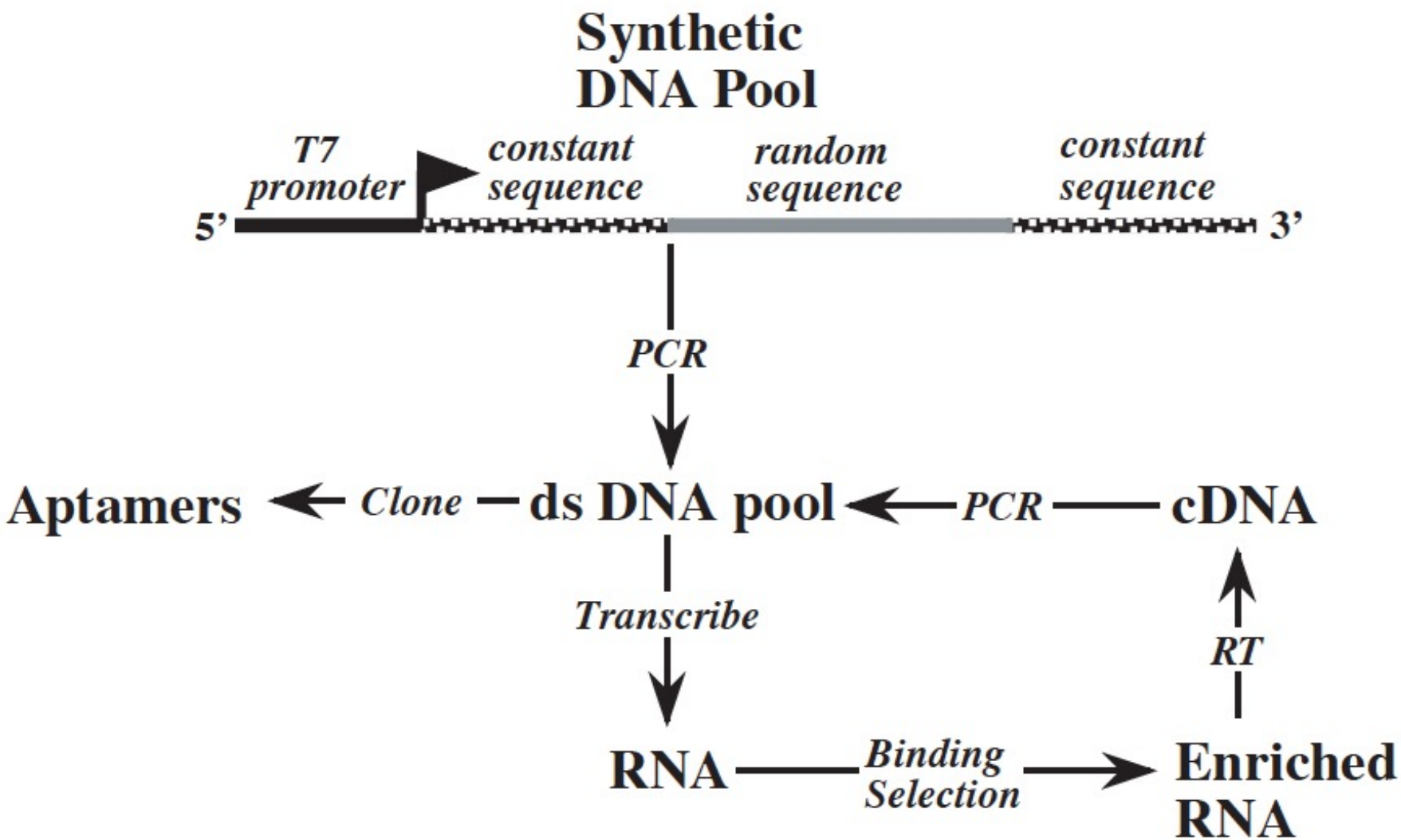

Table 1 (*Continued*)

Target for aptamer selection	Type of aptamer	K_D	References
Ricin toxin	DNA	58–105 nmol/L	Tang et al. (2006)
Cholic acid	DNA	5–67.5 μmol/L	Kato et al. (2000)
4,4′-Methylenedianiline	RNA	0.45–15 μmol/L	Brockstedt et al. (2004)
Dopamine	RNA	2.8 μmol/L	Mannironi et al. (1997)
Cocaine	DNA	n.s.[a]	Stojanovic et al. (2000)
Nucleotides and derivatives			
Adenine	RNA	10 μmol/L	Meli et al. (2002)
ATP (adenosine)	RNA	0.7–50 μmol/L	Sassanfar and Szostak (1993)
Adenosine/ATP	DNA	6 μmol/L	Huizenga and Szostak (1995)
ATP	RNA	4.8–11 μmol/L	Sazani et al. (2004)
Xanthine	RNA	3.3 μmol/L	Kiga et al. (1998)
cAMP	RNA	10 μmol/L	Koizumi and Breaker (2000)
Cofactors			
Coenzyme A	RNA	n.s.[a]	Saran et al. (2003)
Cyanocobalamin	RNA	88 nmol/L	Lorsch and Szostak (1994)
Riboflavin	RNA	1–5 μmol/L	Lauhon and Szostak (1995)
FMN	RNA	0.5 μmol/L	Burgstaller and Famulok (1994)
FAD	RNA	137–273 μmol/L	Burgstaller and Famulok (1994)
NAD	RNA	n.s.[a]	Burgstaller and Famulok (1994)
	RNA	2.5 μmol/L	Lauhon and Szostak (1995)
S-adenosyl methionine	RNA	n.s.[a]	Burke and Gold (1997)
S-adenosyl homocysteine	RNA	0.1 μmol/L	Gebhardt et al. (2000)
Biotin	RNA	5 μmol/L	Wilson et al. (1998) and Wilson and Szostak (1995)
Nucleic acids			
TAR RNA element of HIV-1	DNA	50 nmol/L	Boiziau et al. (1999)
	RNA	20–50 nmol/L	Duconge and Toulme (1999)
	DNA	50 nmol/L	Sekkal et al. (2002)
Yeast phenylalanine tRNA	RNA	12–26 nmol/L	Scarabino et al. (1999)
E.coli 5S RNA	RNA	6–12 μmol/L	Ko et al. (1999)
	RNA	3 μmol/L	Ko et al. (2001)
Amino acids			
L-Arginine	RNA	330 nmol/L	Geiger et al. (1996)
	DNA	~2.5 mmol/L	Harada and Frankel (1995)
L-Citrulline	RNA	62–68 μmol/L	Famulok (1994)
L-Valine	RNA	12 mmol/L	Majerfeld and Yarus (1994)
L-Isoleucine	RNA	1–7 mmol/L	Lozupone et al. (2003)
	RNA	200–500 μmol/L	Majerfeld and Yarus (1998)
D-Tryptophan	RNA	18 μmol/L	Famulok and Szostak (1992)
L-tyrosinamide	DNA	45 μmol/L	Vianini et al. (2001)
L-histidine	RNA	8–54 μmol/L	Majerfeld et al. (2005)
Carbohydrates			
Cellobiose	DNA	600–nmol/L	Yang et al. (1998)
Sialyl Lewis X	RNA	0.085–10 nmol/L	Jeong et al. (2001)
Chitin	DNA	n.s.[a]	Fukusaki et al. (2000)
Sialyllactose	DNA	4.9 μmol/L	Masud et al. (2004)
Sephadex	DNA	n.s.[a]	Srisawat et al. (2001)
Antibiotics			
Kanamycin A	RNA	≤300 nmol/L	Lato et al. (1995)
Kanamycin B	RNA	180 nmol/L	Kwon et al. (2001)
Streptomycin	RNA	n.s.[a]	Wallace and Schroeder (1998)
Neomycin	RNA	~100 nmol/L	Wallis et al. (1995)
Tobramycin	RNA	2–3 nmol/L	Wang and Rando (1995)
Lividomycin	RNA	≤300 nmol/L	Lato et al. (1995) and Lato and Ellington (1996)
Moenomycin A	RNA	300–400 nmol/L	Schürer et al. (2001)
Tetracycline	RNA	1 μmol/L	Berens et al. (2001)
Chloramphenicol	RNA	25–65 μmol/L	Burke et al. (1997)
Peptides and proteins			
T4 DNA polymerase	RNA	5–30 nmol/L	Tuerk and Gold (1990)

http://www.ncbi.nlm.nih.gov/pubmed/17627883

RNA Mimics of Green Fluorescent Protein

Jeremy S. Paige,[1] Karen Y. Wu,[1] Samie R. Jaffrey[1,2]*

Green fluorescent protein (GFP) and its derivatives have transformed the use and analysis of proteins for diverse applications. Like proteins, RNA has complex roles in cellular function and is increasingly used for various applications, but a comparable approach for fluorescently tagging RNA is lacking. Here, we describe the generation of RNA aptamers that bind fluorophores resembling the fluorophore in GFP. These RNA-fluorophore complexes create a palette that spans the visible spectrum. An RNA-fluorophore complex, termed Spinach, resembles enhanced GFP and emits a green fluorescence comparable in brightness with fluorescent proteins. Spinach is markedly resistant to photobleaching, and Spinach fusion RNAs can be imaged in living cells. These RNA mimics of GFP provide an approach for genetic encoding of fluorescent RNAs.

Fig. 1. RNA aptamers switch on the fluorescence of GFP-like fluorophores. (**A**) Structures of HBI (green), in the context of GFP, and DMHBI. (**B**) 13-2 enhances the fluorescence of DMHBI. Solutions containing DMHBI, 13-2 RNA, DMHBI with 13-2 RNA, or DMHBI with total HeLa cell RNA were photographed under illumination with 365 nm of light. The image is a montage obtained under identical image-acquisition conditions.

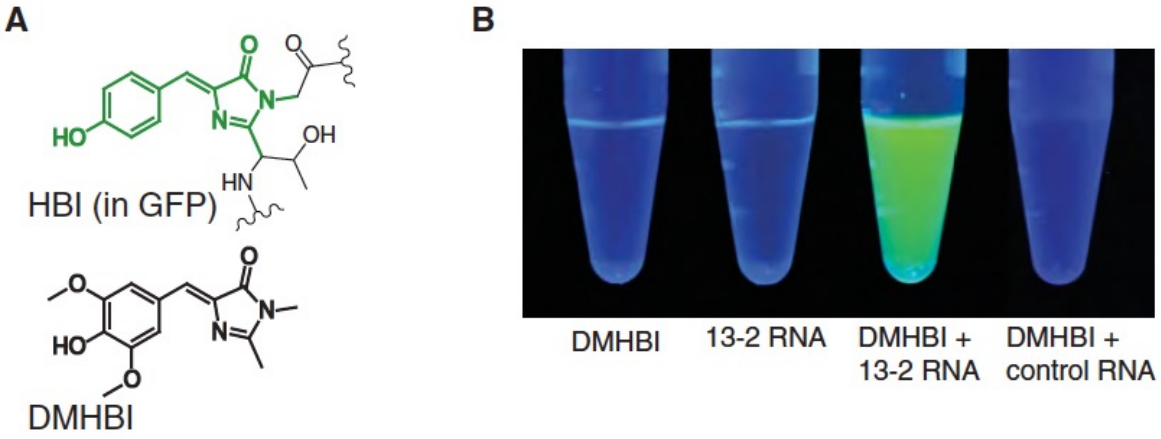

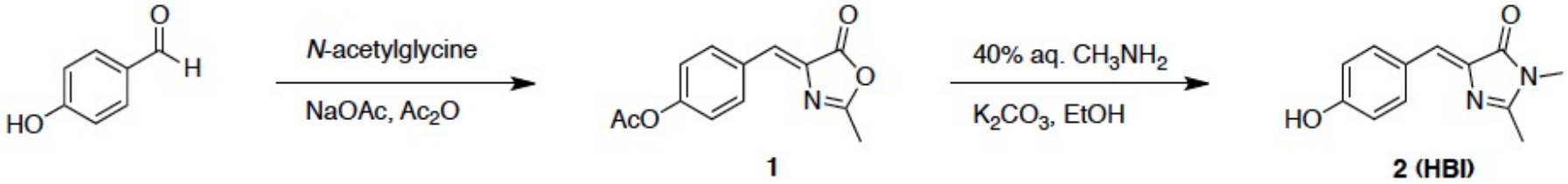

Scheme 1

Table S1 Photophysical and binding properties of RNA-fluorophore complexes

Fluorophore	Excitation maximum (nm)	Emission maximum (nm)	Extinction coefficient ($M^{-1}cm^{-1}$)[a]	Fluorescence quantum yield	K_D	Brightness[b]
Aequorea GFP[c]	395	508	27,600	0.79	-	100
EGFP[c]	489	508	55,000	0.60	-	151
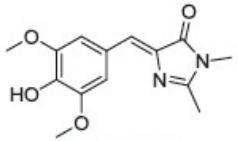 DMHBI	394	487	23,336	0.0005	-	0.05
2-4	397	464	21,536	0.10	N.D.[d]	6
13-2	398	529	23,391	0.06	464 nM	12
13-2-min	398	529	23,391	0.11	N.D.	12
3-6	398	537	25,300	0.05	406 nM	6
17-3	405	547	18,127	0.09	N.D.	7
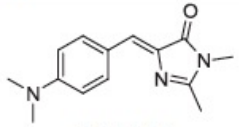 DMABI	447	519	14,329	0.003	-	0.2
11-3	489	512	18,743	0.05	N.D.	4
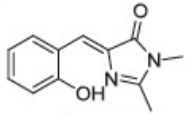 2-HBI	399	461	10,943	0.0005	-	0.02
6-8	396	588	10,714	0.004	N.D.	0.2
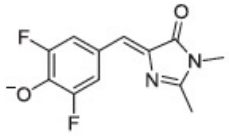 DFHBI	405	498	11,864	0.0007	-	0.04
24-2 (Spinach)	469	501	24,271	0.72	537 nM	80

[a]Extinction coefficients for fluorophores alone were measured at a pH in which all species were in the phenolic form except for DFHBI which was measured in its phenolate form. RNA-fluorophore complex extinction coefficients were all measured at pH 7.4. [b]Brightness (extinction coefficient × quantum yield) is reported relative to *Aequorea* GFP. [c]See reference 40. [d]N.D. = not determined.

E

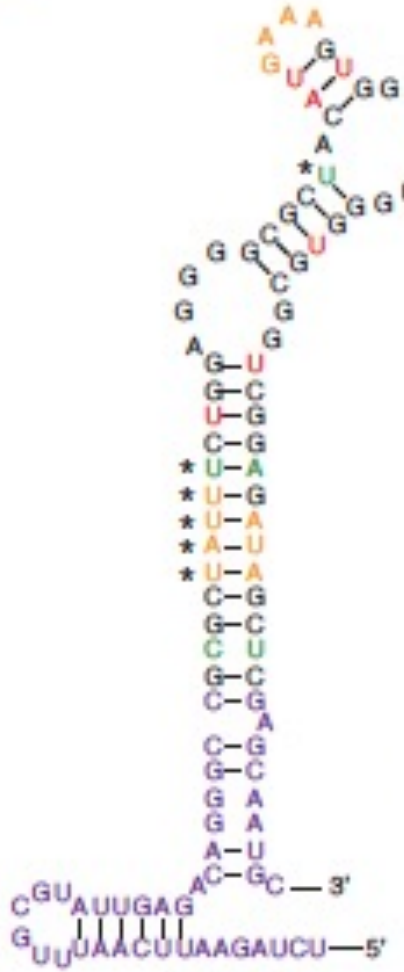

13-2

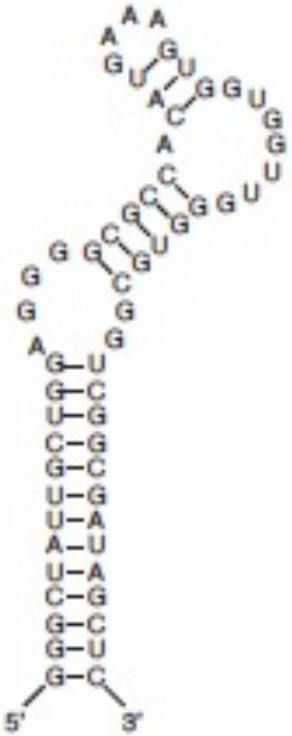

13-2-min

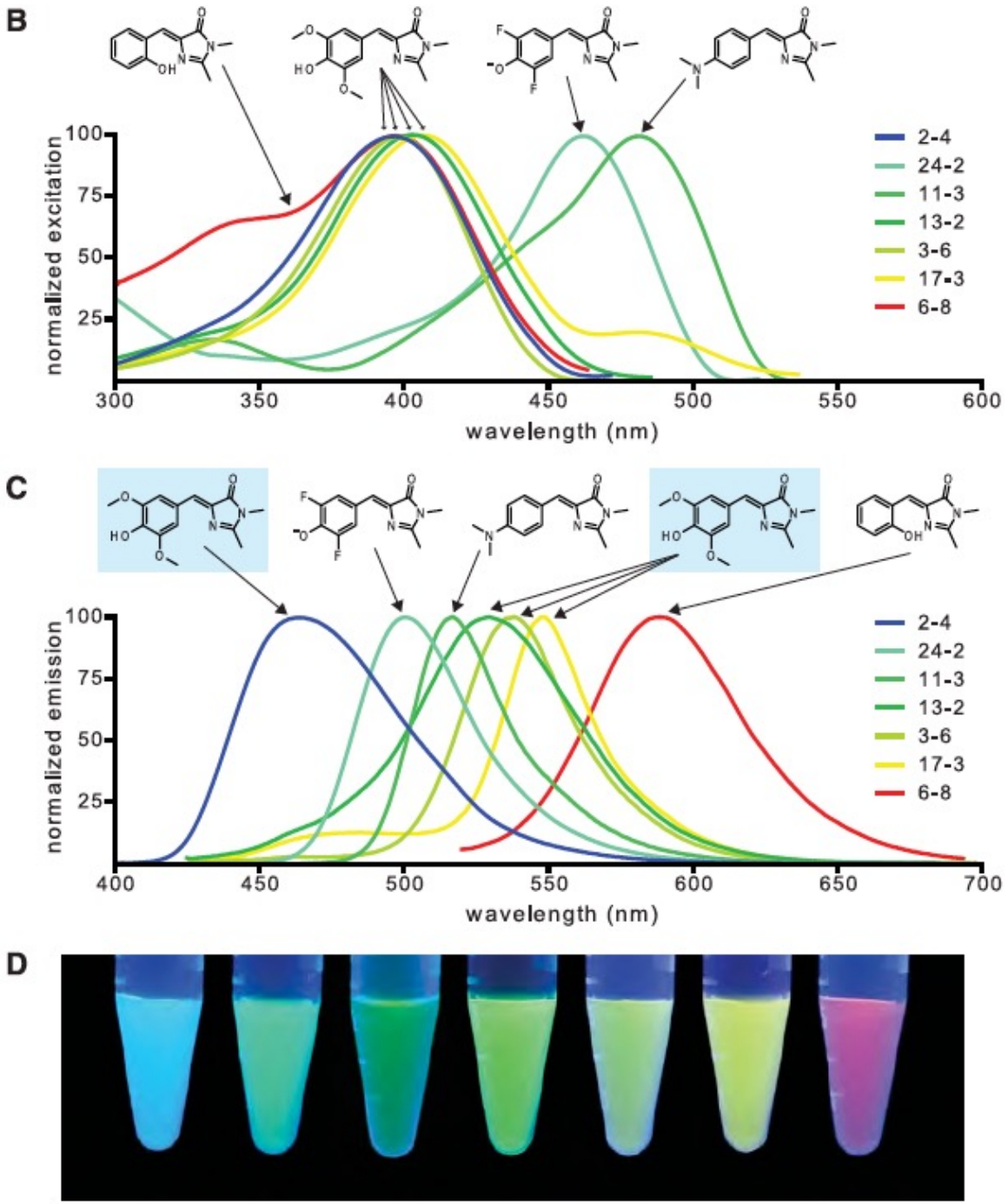
B
normalized excitation
100
75
50
25
300
350
400
450
500
550
600
wavelength (nm)
2-4
24-2
11-3
13-2
3-6
17-3
6-8
C
normalized emission
100
75
50
25
400
450
500
550
600
650
700
wavelength (nm)
2-4
24-2
11-3
13-2
3-6
17-3
6-8
D

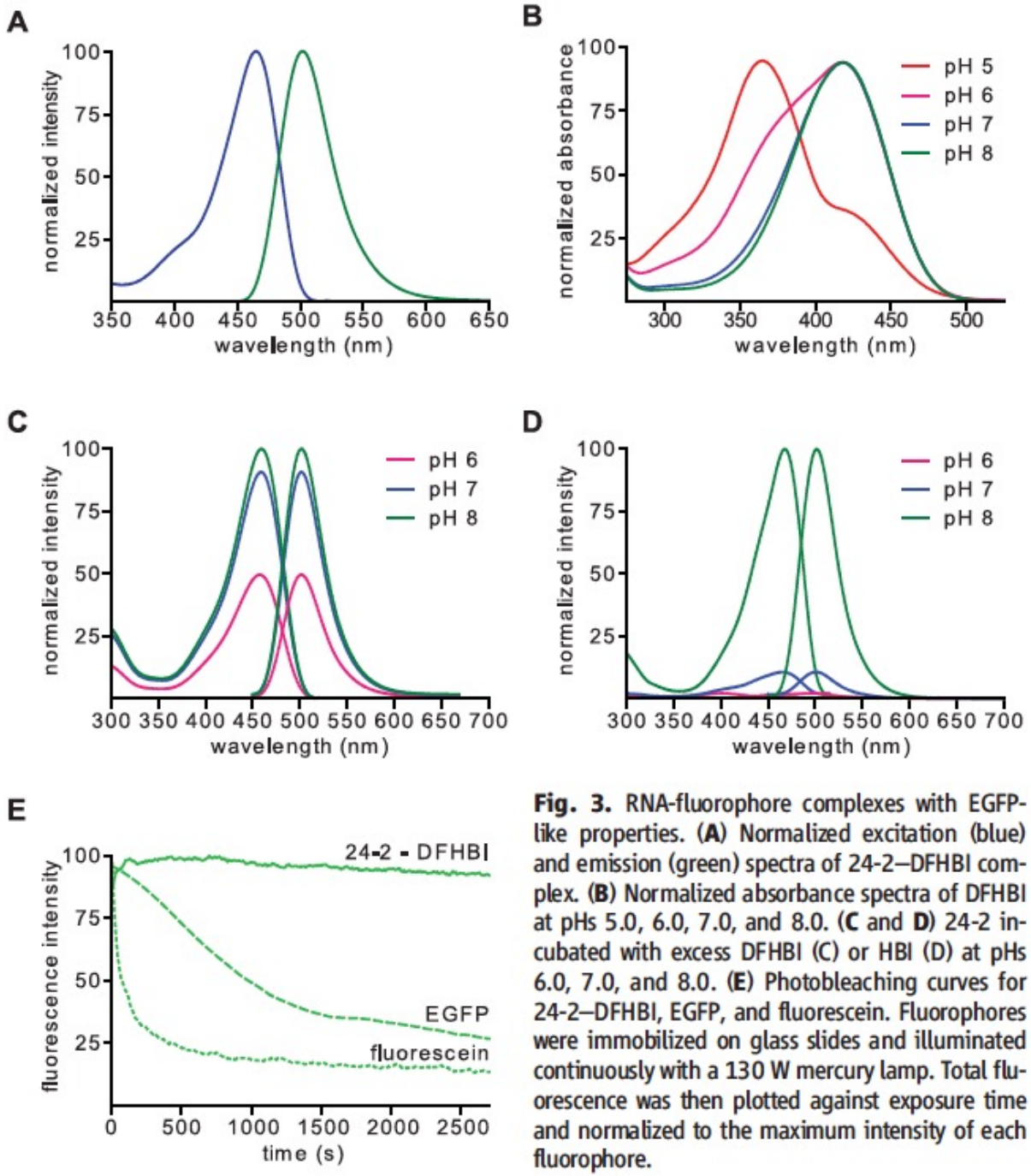

Fig. 3. RNA-fluorophore complexes with EGFP-like properties. (**A**) Normalized excitation (blue) and emission (green) spectra of 24-2–DFHBI complex. (**B**) Normalized absorbance spectra of DFHBI at pHs 5.0, 6.0, 7.0, and 8.0. (**C** and **D**) 24-2 incubated with excess DFHBI (C) or HBI (D) at pHs 6.0, 7.0, and 8.0. (**E**) Photobleaching curves for 24-2–DFHBI, EGFP, and fluorescein. Fluorophores were immobilized on glass slides and illuminated continuously with a 130 W mercury lamp. Total fluorescence was then plotted against exposure time and normalized to the maximum intensity of each fluorophore.

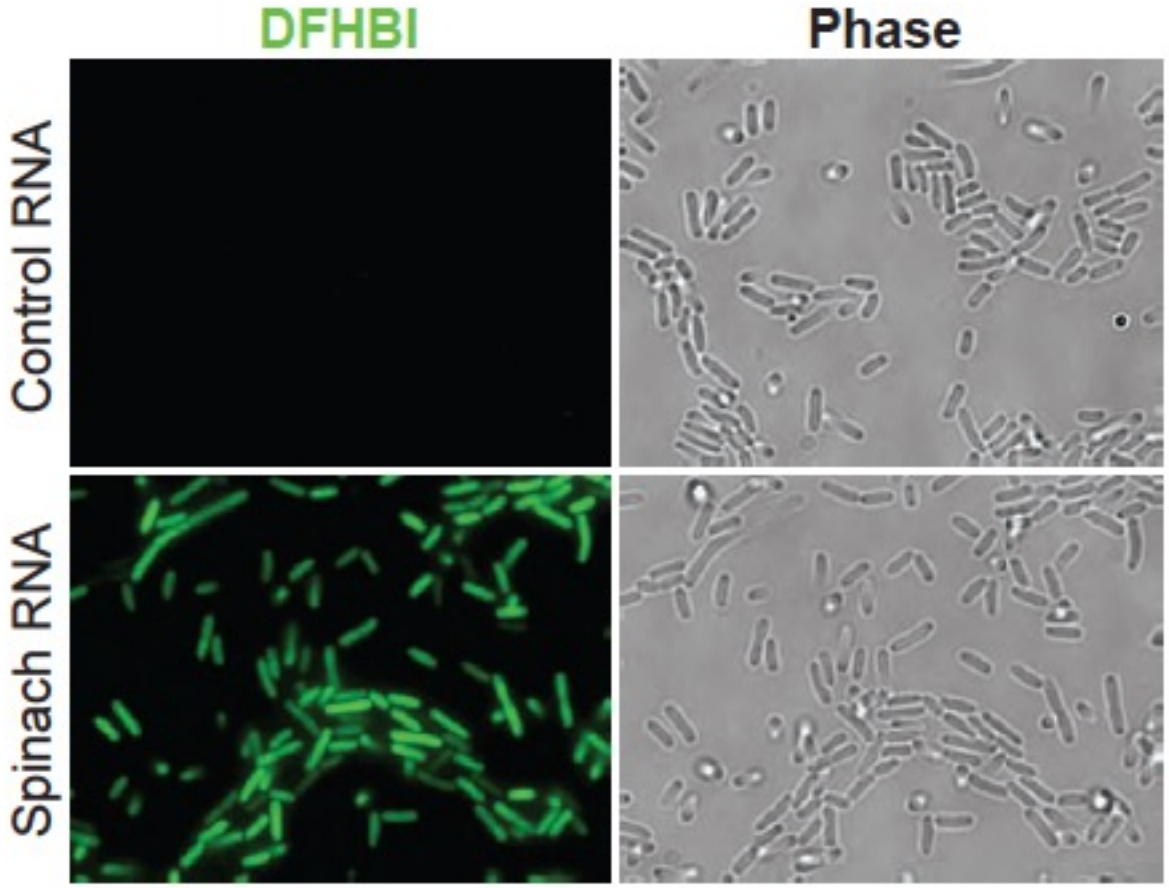
DFHBI
Phase
Control RNA
Spinach RNA

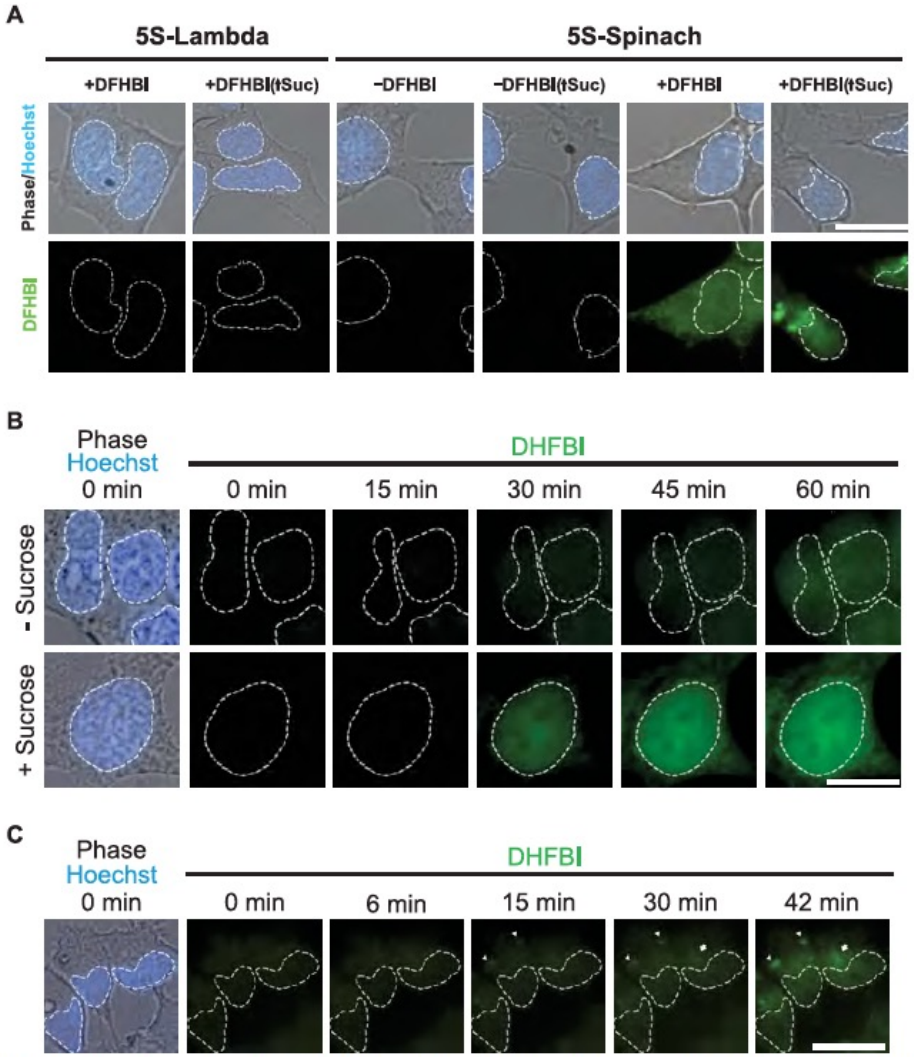

Fig. 4. Live-cell imaging of Spinach fusion RNAs. (**A**) Live-cell imaging of Spinach-tagged 5*S* RNA. Fluorescence and phase images of HEK293 T cells expressing 5*S* tagged with either Spinach or Lambda, a control RNA. Fluorescence is detected in 5*S*-Spinach–expressing cells in the presence of 20 μM DFHBI, with granule formation present in cells treated with 600 mM sucrose for 30 min (↑Suc). White dashed lines indicate nuclear borders assessed by means of Hoescht 33342 staining. (**B**) 5*S*-Spinach RNA induction in response to stress. 5*S*-Spinach–expressing HEK293 T cells were pretreated with 30 nM ML-60128 for 16 hours and then treated with vehicle or 600 mM sucrose for 60 min. Treatment of cells with sucrose resulted in a rapid induction of 5*S*-Spinach RNA and an increase in total 5*S*-Spinach levels compared with control cells. (**C**) 5*S*-Spinach RNA localization into granules. 5*S*-Spinach–expressing HEK293 T cells were stimulated with 600 mM sucrose in order to monitor the rate of formation of 5*S*-Spinach–containing granules. Arrowheads indicate granules that formed earliest, and arrows indicate granules that developed later during the time course of treatment. Scale bar, 10 μm.

Fig. 1 Imaging SAM in living cells with RNA. (A) The sensor RNA comprises Spinach (black), a transducer (orange), and a target-binding aptamer (blue).

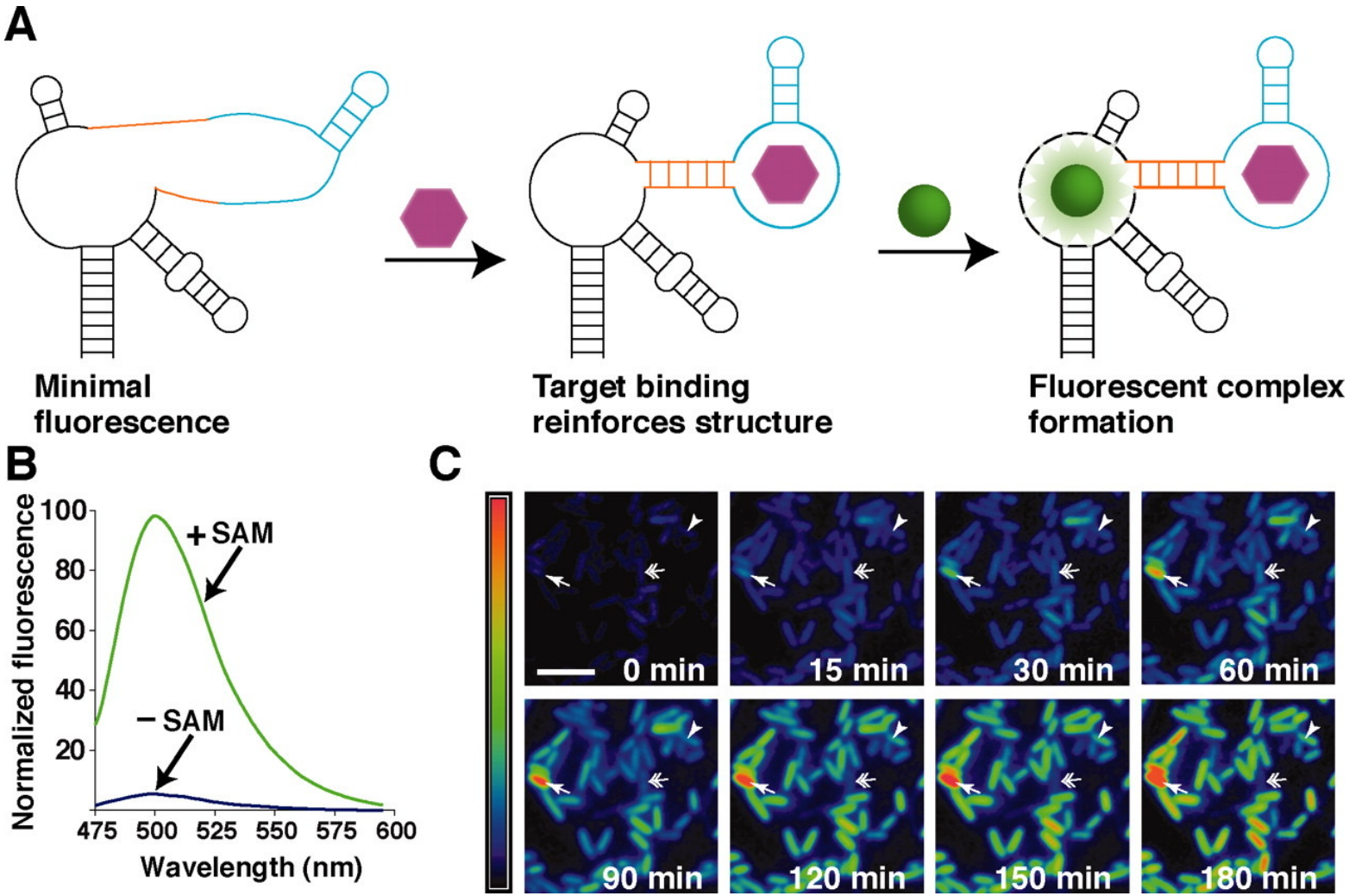

Jeremy S. Paige et al. Science 2012;335:1194

Goal of DNA imaging:

Time-resolved, 3D positions of the entire genome, with information on sequence and epigenetic modification.

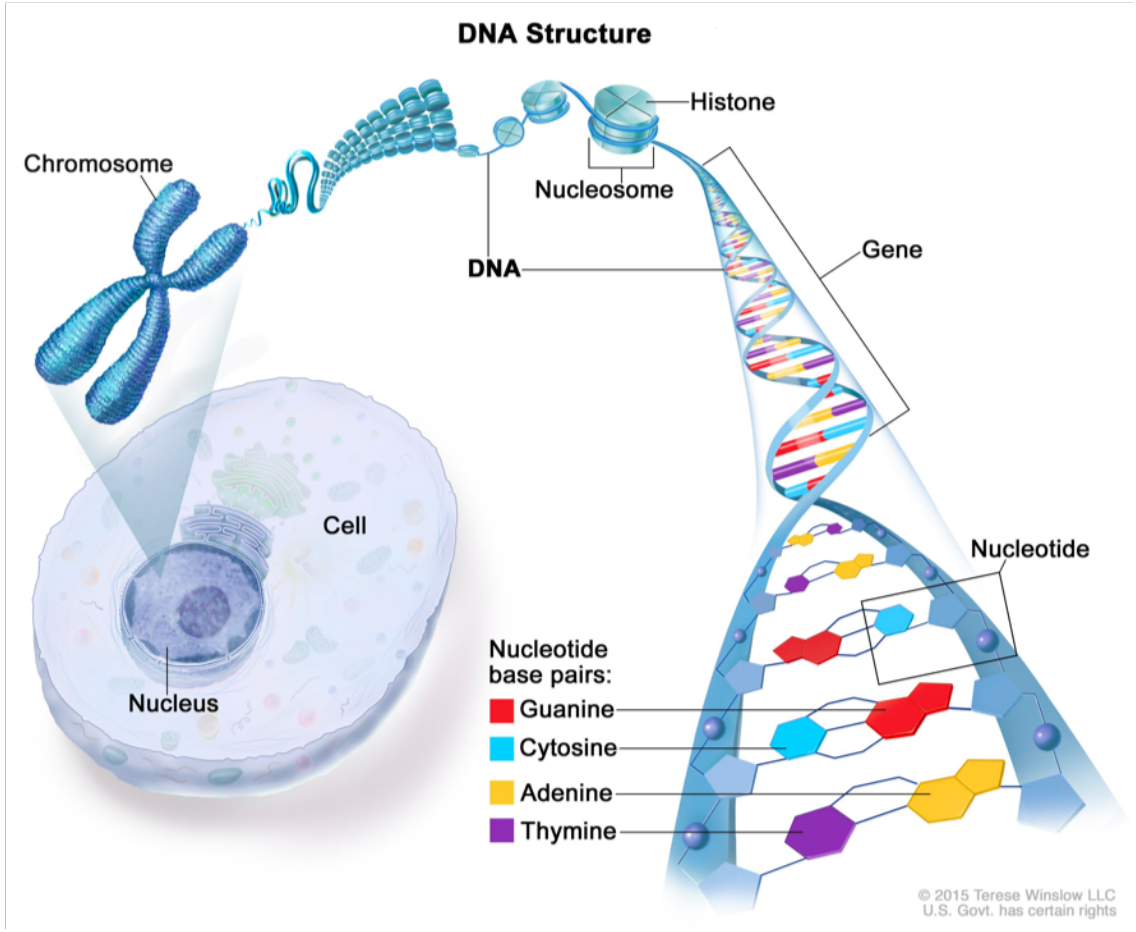

https://www.cancer.gov/about-nci/organization/ccg/research/structural-genomics/tcga, 29/5/2020

Outline

1. Why should we study DNA in cells?
2. DNA labeling methods:
   a) DNA dye staining
   b) Unnatural nucleosides and pro-nucleotides
   c) CASFISH – a CRISPR-dCas9 method
3. Paper

   Rieder et al. – Alkene-Tetrazine Ligation for Imaging Cellular DNA

1. DNA is involved in many cellular processes that occur on a time scale that can be observed with common imaging techniques

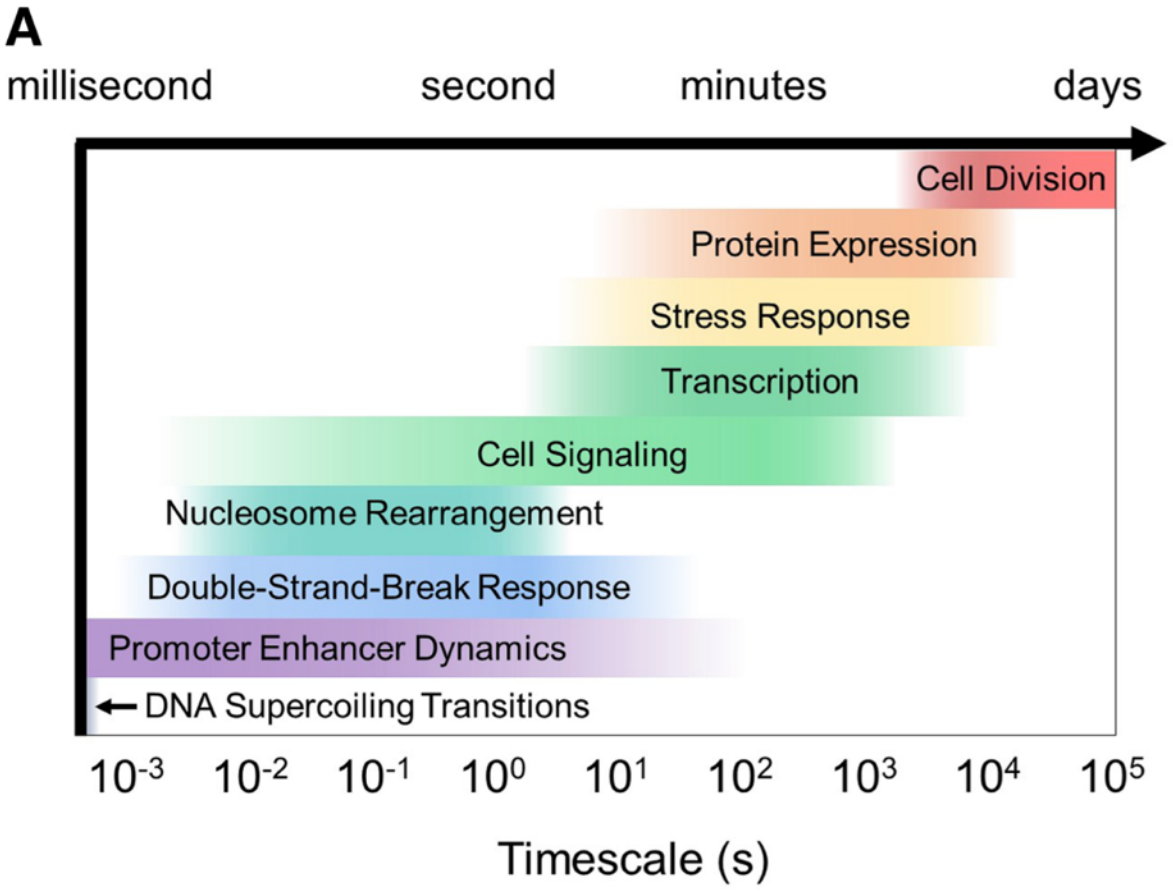

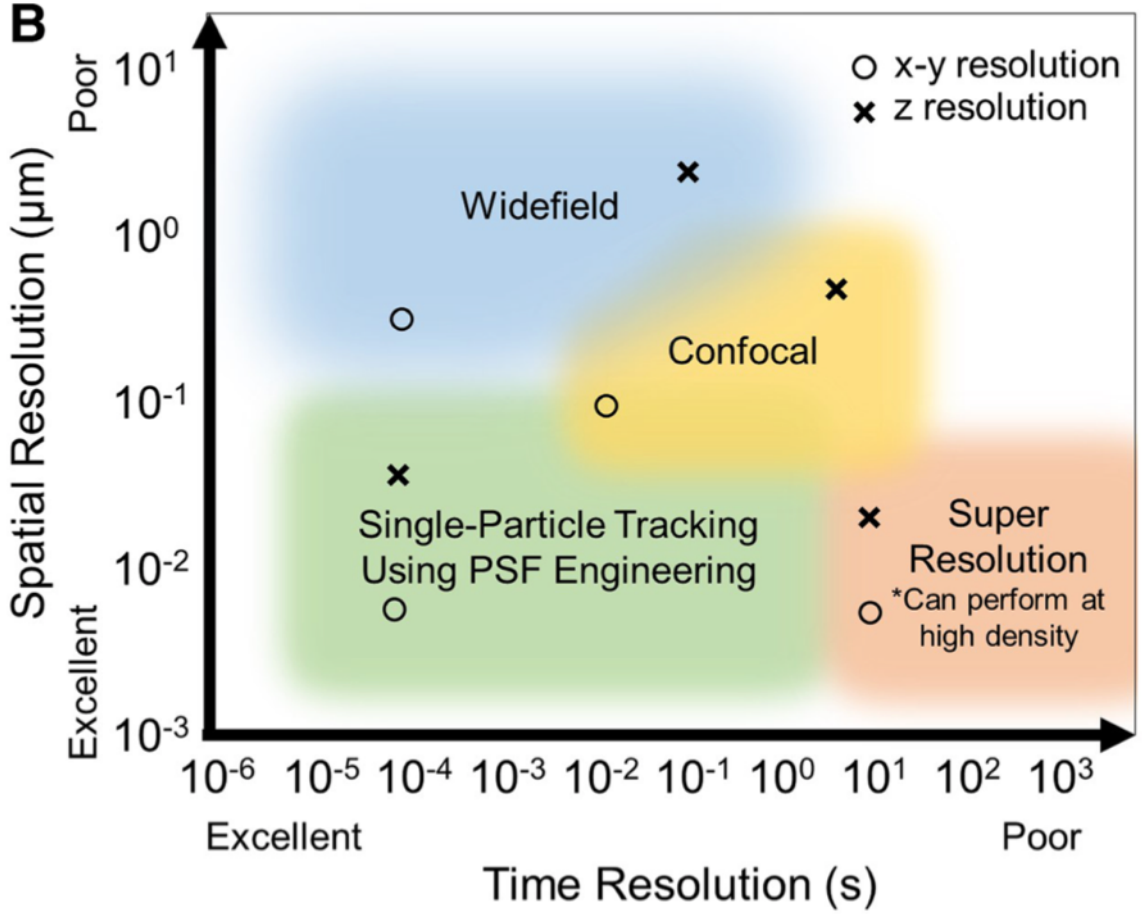

Biochem. Soc. Trans. **2018**, *46*, 729–740.

MAX-PLANCK-GESELLSCHAFT

1. Questions that could be addressed with DNA imaging

- To what extent does the structuring of chromatin in topological regions (e.g., chromatin domains) contribute to nuclear functioning? On what length scales does this structuring occur?
- How is it dynamically organized e.g., during the cell cycle or during DNA replication or transcription?
- How are the dynamical processes themselves responsible for the possibly induced structural changes of chromatin?

Genes **2019**, *10*, 493.

1. Key applications of DNA imaging

Application	Labeling method
Cell viability test	Cell impermeable DNA stain
Imaging chromatin	Cell permeable DNA stain
Cell cycle analysis, DNA replication and repair	DNA stain, Unnatural nucleosides or pro-nucleotides
Tracking repetitive loci	DNA binding proteins (Zinc finger proteins)
Tracking specific, nonrepetitive loci	DNA binding proteins (CRISPR-dCas9 method)

2. DNA labeling methods: a) DNA dye staining

- Intercalating between base pairs
  - Cyanine monomers and dimers (Mono- and bisintercalator)
  - Phenanthridines and acridines

- Minor groove binder
  - Indoles and imidazoles

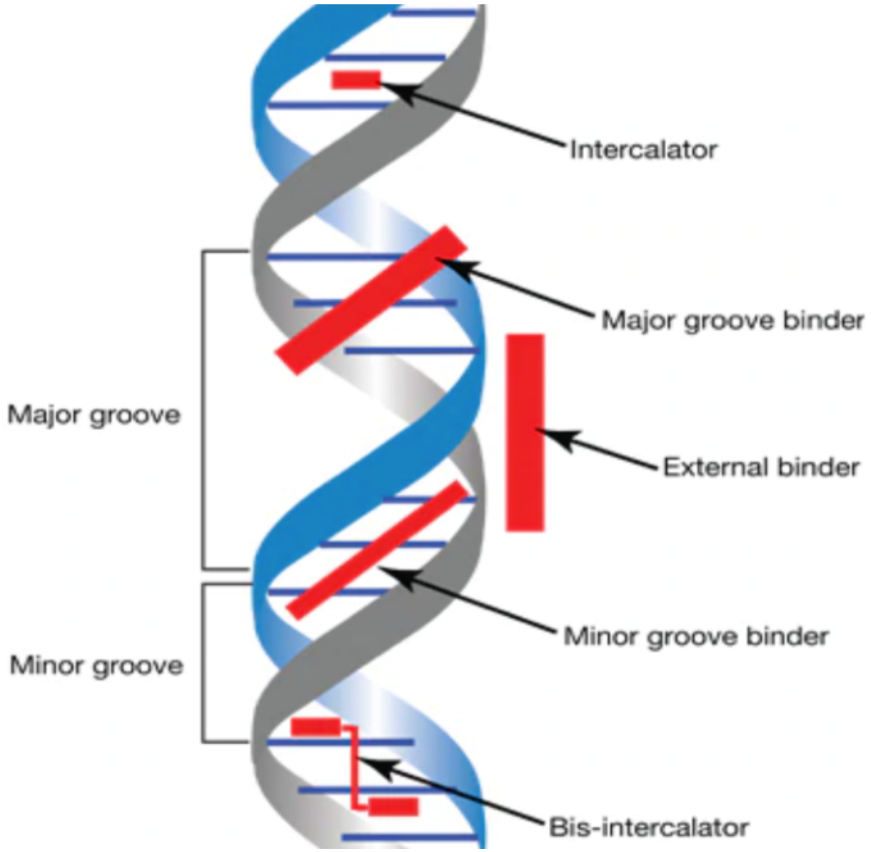

https://www.thermofisher.com/de/de/home/references/molecular-probes-the-handbook/nucleic-acid-detection-and-genomics-technology/nucleic-acid-stains.html, 29/5/20

2. DNA labeling methods: a) DNA dye staining

Cyanine Dyes:

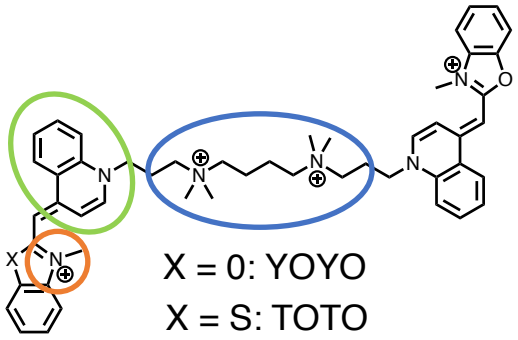

X = 0: YOYO
X = S: TOTO

YO = Oxazole Yellow,
TO = Thiazole Orange

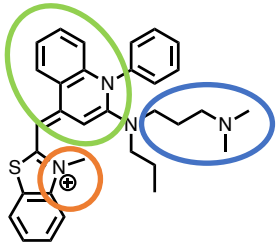

SYBR Green

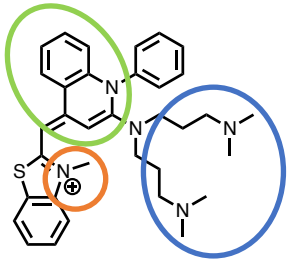

Pico Green

- Intercalator
- Interaction with phosphate backbone
- Interaction with DNA minor groove

Properties:

- High turn-on upon DNA binding
- Mostly cell impermeable

Applications:

- Ultrasensitive nucleic acid detection and quantification in solution or gels
- Dead-live stain to determine cell cytotoxicity

2. DNA labeling methods: a) DNA dye staining

Classical Intercalators: phenanthrines and acridines

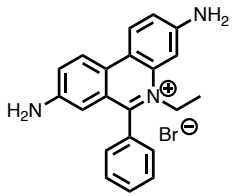

Ethidium bromide (EtBr)

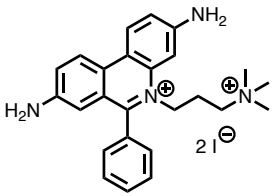

Propidium iodide (PI)

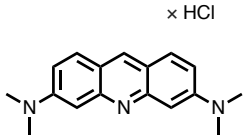

Acridine orange

Properties:

- EtBr and PI are potent mutagens.
- Acridine orange has an emission maximum at 525 nm when bound to DNA that is shifted to 650 nm when bound to RNA.

Applications:

- PI is a commonly used as chromosome and nuclear counterstain *e. g.* in flow cytometry.
- Acridine Orange is a dual-fluorescence nucleic acid stain that can be used for RNA/DNA discrimination measurements.

2. DNA labeling methods: a) DNA dye staining

Minor groove binders: Indoles and Imidazoles

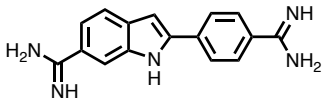

DAPI

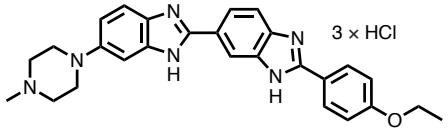

Hoechst33342

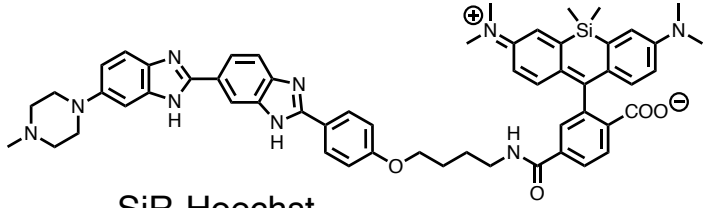

SiR-Hoechst

Properties:

- AT-selective.
- DAPI is cell-impermeable whereas Hoechst33342 and SiR-Hoechst are cell peremable.

Applications:

- Nuclear counterstains for fluorescence microscopy.
- Cell cycle analysis for flow cytometry or fluorescence microscopy.

2. DNA labeling methods: a) DNA dye staining can give super-resolved images of chromatin

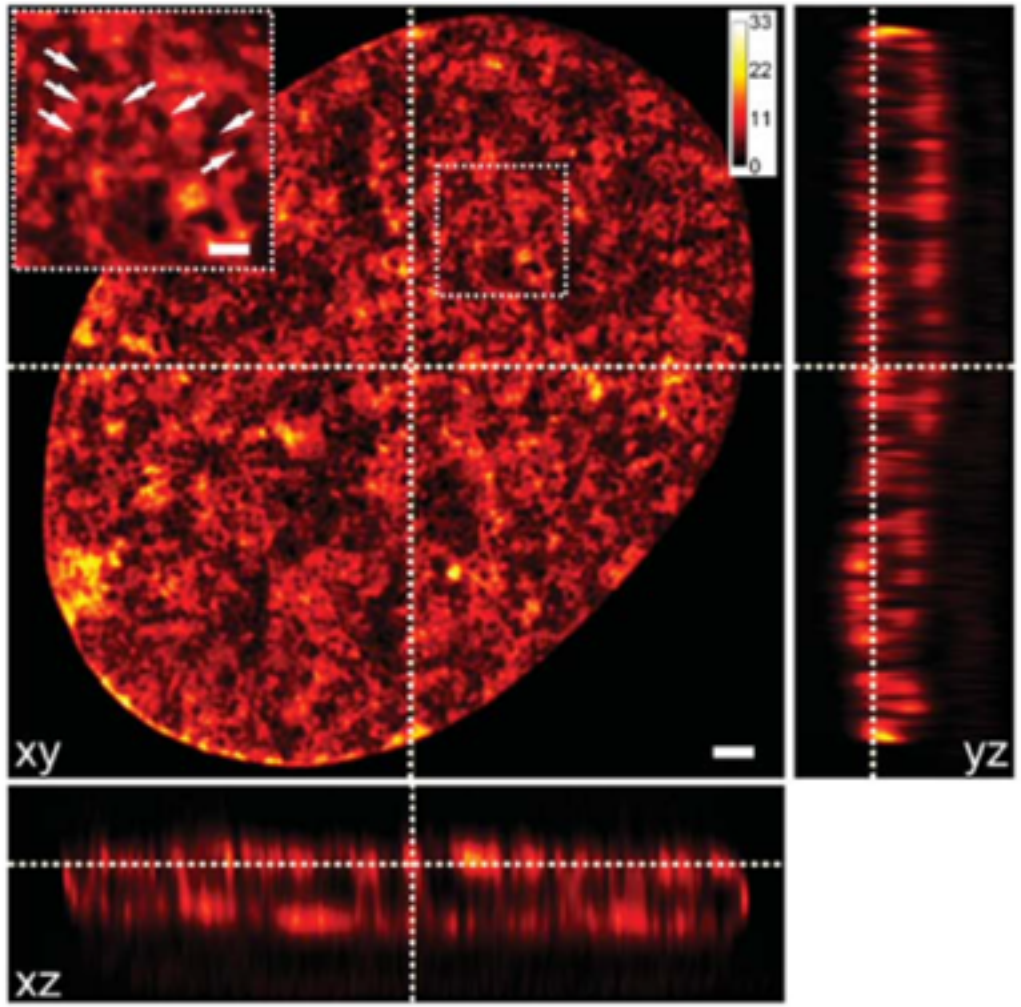

STED nanoscopy images of nuclei in living fibroblast stained 5-610CP-Hoechst. Arrows indicate heterochromatin exclusion zones (HEZs). Scale bar: 1 mm in the large image and 0.5 mm in the inset.

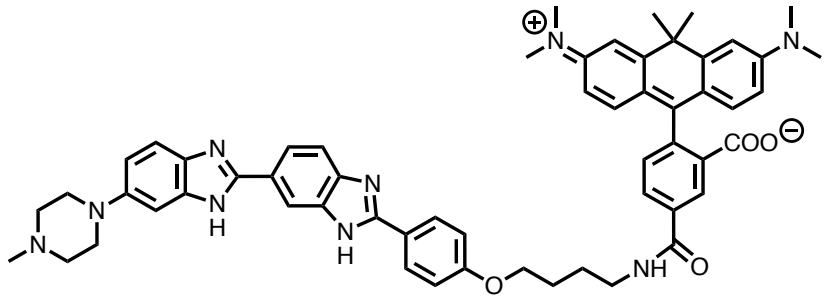

Chem. Sci. **2019**, *10*, 1962–1970.

2. DNA labeling methods: b) Labeling newly synthesized DNA

(i) Metabolic processing of nucleoside or pro-nucleotide analogues in living cells.

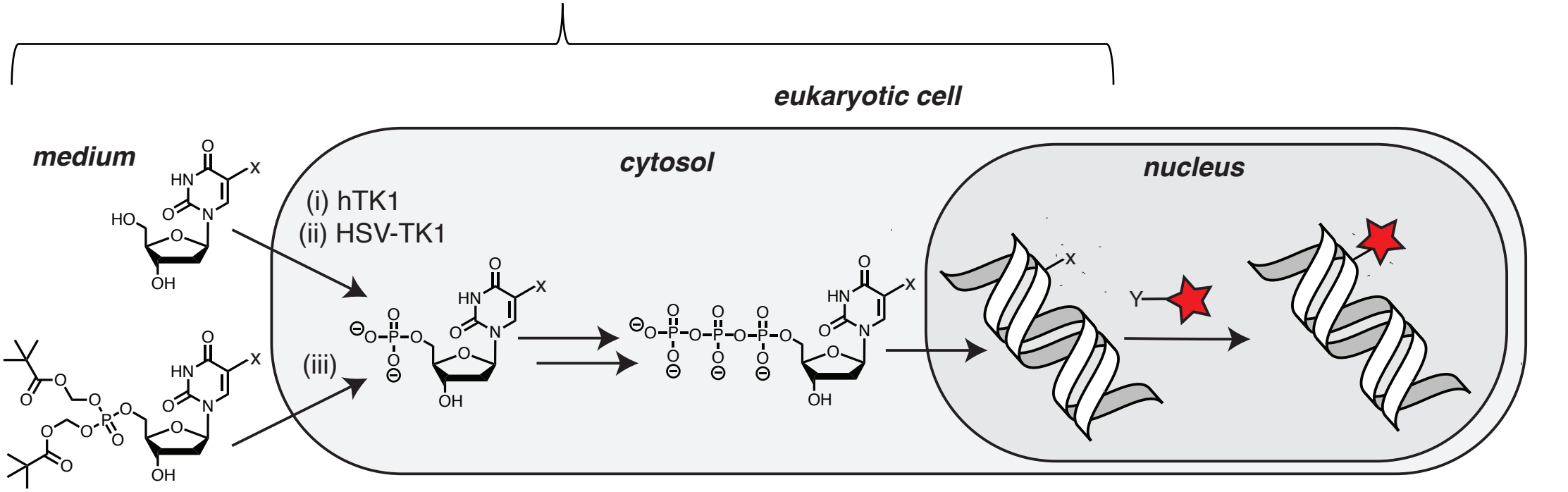

TK = thymidine kinase
h = human
HSV = herpes simplex virus

(ii) Visualization with fluorophores in fixed cells.

2. DNA labeling methods: b) Labeling newly synthesized DNA: Unnatural nucleosides

5-Bromo-2‘-deoxyuridine (BrdU)

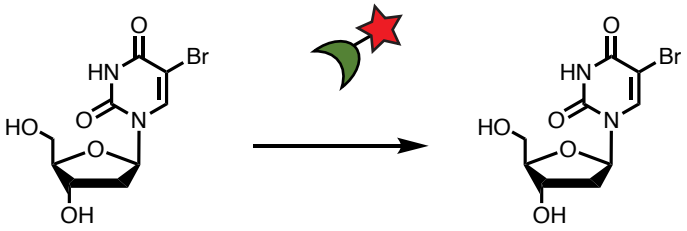

Immunostaining with antibody

5-Ethynyl-2‘-deoxyuridine (EdU)

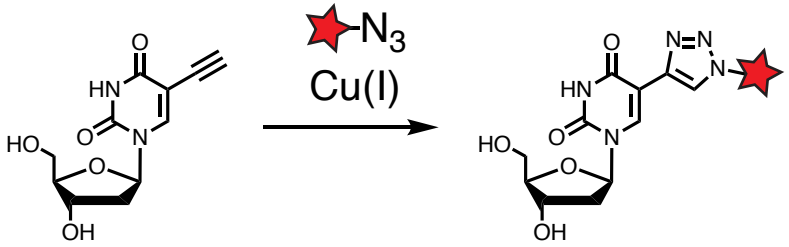

Cupper-catalyzed azide-alkyne cycloaddition (CuAAC)

$k \sim 10 – 200\ M^{-1}\ s^{-1}$

5-Vinyl-2‘-deoxyuridine (VdU)

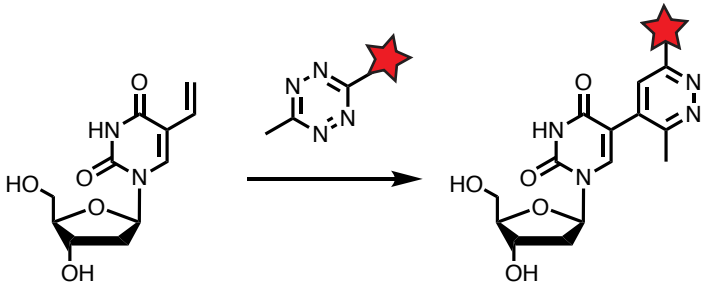

Inverse electron-demand Diels Alder reaction (iEDDA)

$k_{VdU} \sim 0.021\ M^{-1}\ s^{-1}$, (other dienophiles: $k_{tetrazines} \sim 1 - 10^4\ M^{-1}\ s^{-1}$)

Hum Genet **1986**, *72*, 129-132.
Proc Natl Acad Sci USA **2008**, *105*, 2415-20.
Angew Chem Int Ed Engl **2014**, *53*, 9168-72.
ACS Chem. Biol. **2014**, *9*, 16–20.

2. DNA labeling methods: b) Labeling newly synthesized DNA: EdU

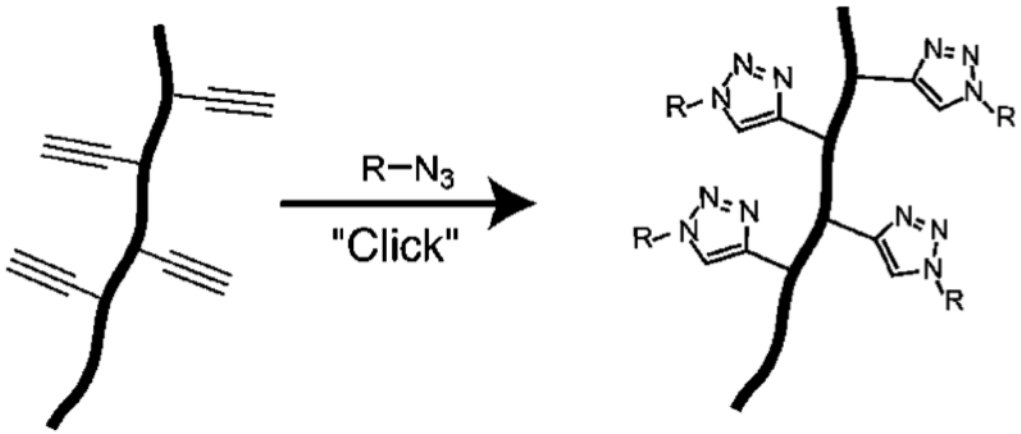

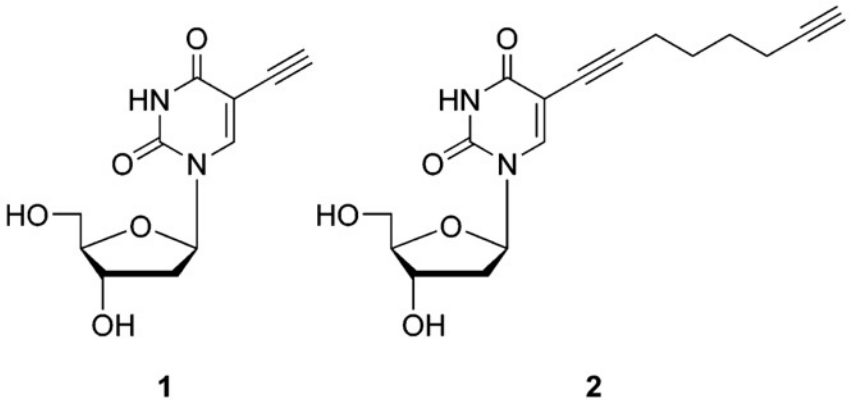

- Postsynthethic modification of oligonucleotides using Cu(I) catalyzed azide-alkyne cycloaddition was first demonstrated by Carell in 2006.
- Applications in mammalian cells were published two years later in 2008.

Org. let. **2006**, *8, 17*, 3639-42.

2. DNA labeling methods: b) Labeling newly synthesized DNA: EdU

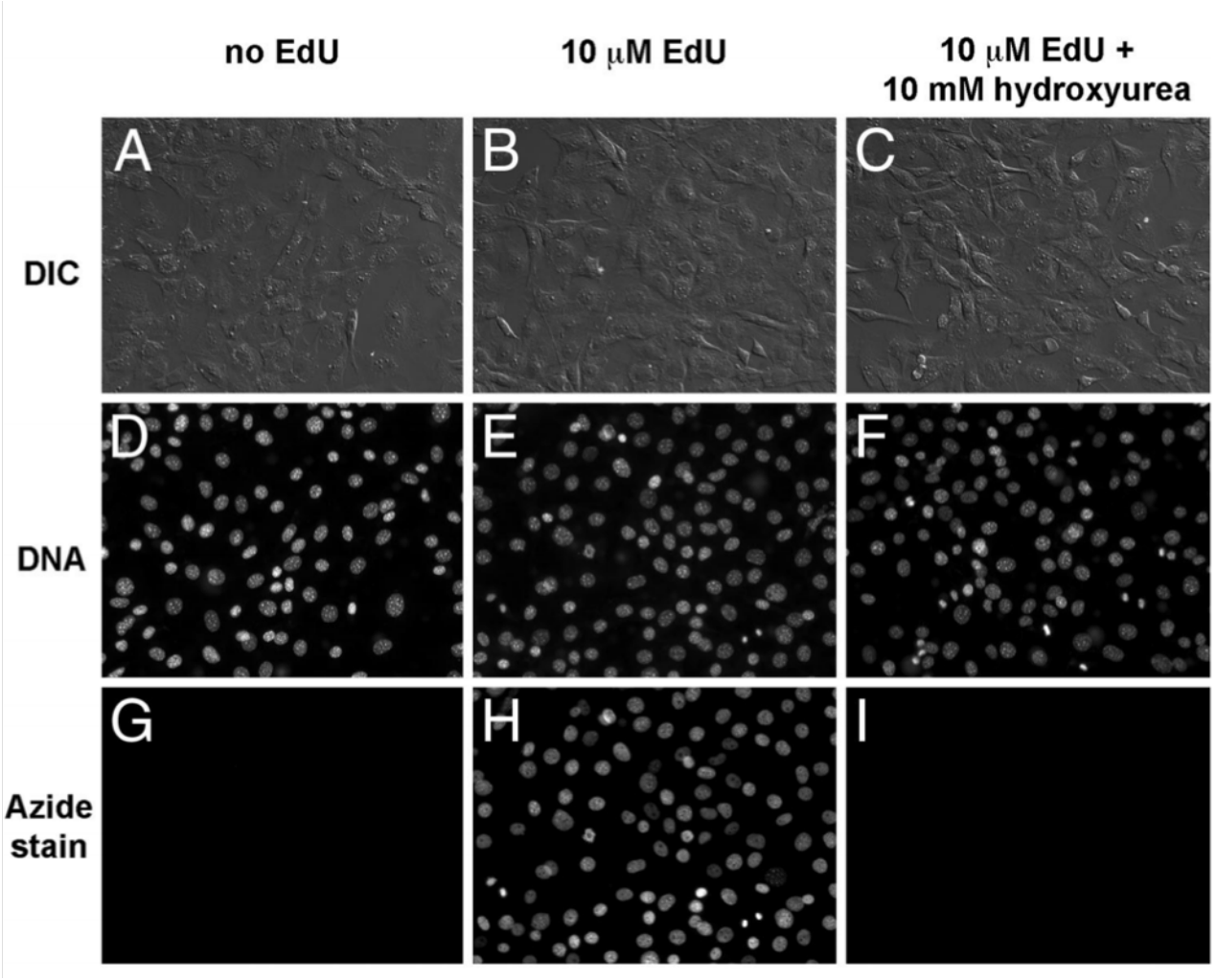

Fig. 2. Detection of EdU incorporated into the DNA of cultured NIH 3T3 cells (*A–M*) and HeLa cells (*N–P*) by fluorescence microscopy. NIH 3T3 cells were incubated in media without EdU (*A*, *D*, *G*, *J*, and *L*), media supplemented with 10 μM EdU (*B*, *E*, and *H*) or media with 10 μM EdU and 10 mM hydroxyurea to block DNA synthesis (*C*, *F*, *I*, *K*, and *M*). In *A–M*, the cells were fixed and then reacted with 10 μM Alexa568-azide (Fig. 1*C*, compound 2) for 10 min. The cells were then counterstained with Hoechst to reveal cellular DNA, washed, and imaged by fluorescence microscopy and differential interference contrast (DIC). Note the strong specific and low nonspecific azide stain in the presence (*H*) and absence (*G*) of EdU, respectively. Not all nuclei in *H* are labeled after overnight incubation with EdU, suggesting that only cells that went through S phase became labeled. Blocking DNA replication with hydroxyurea abolishes EdU incorporation almost completely (*I*).

- EdU incorporation can be diminished with the DNA synthesis inhibitor hydroxyurea.

PNAS **2008**, *105*, 2415-20.

2. DNA labeling methods: b) Labeling newly synthesized DNA: EdU

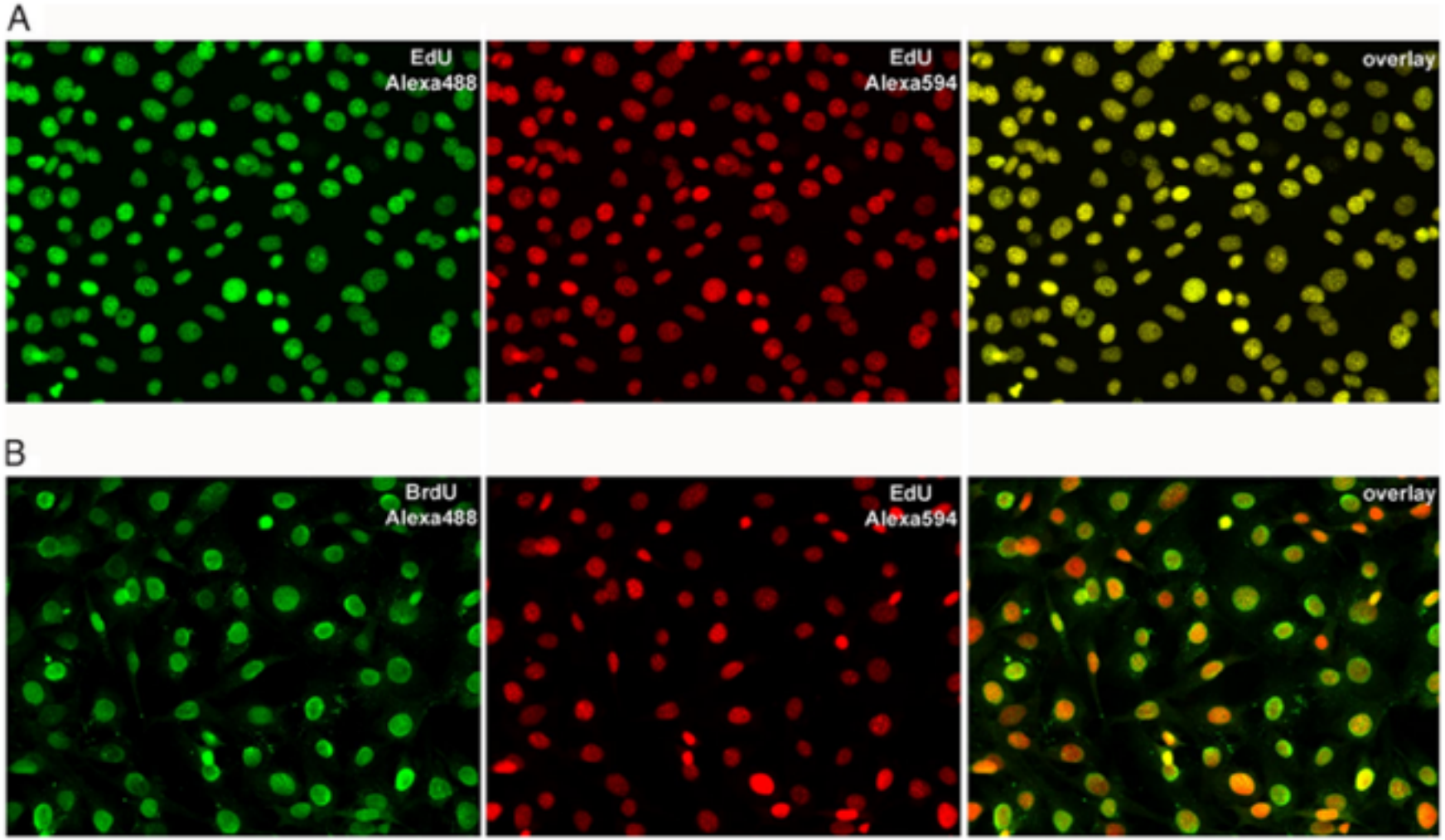

Fig. 3. Reproducibility of EdU labeling (*A*) and comparison with BrdU (*B*)

- EdU signals colocalize with BrdU signals.

PNAS **2008**, *105*, 2415-20.

2. DNA labeling methods: b) Labeling newly synthesized DNA: EdU

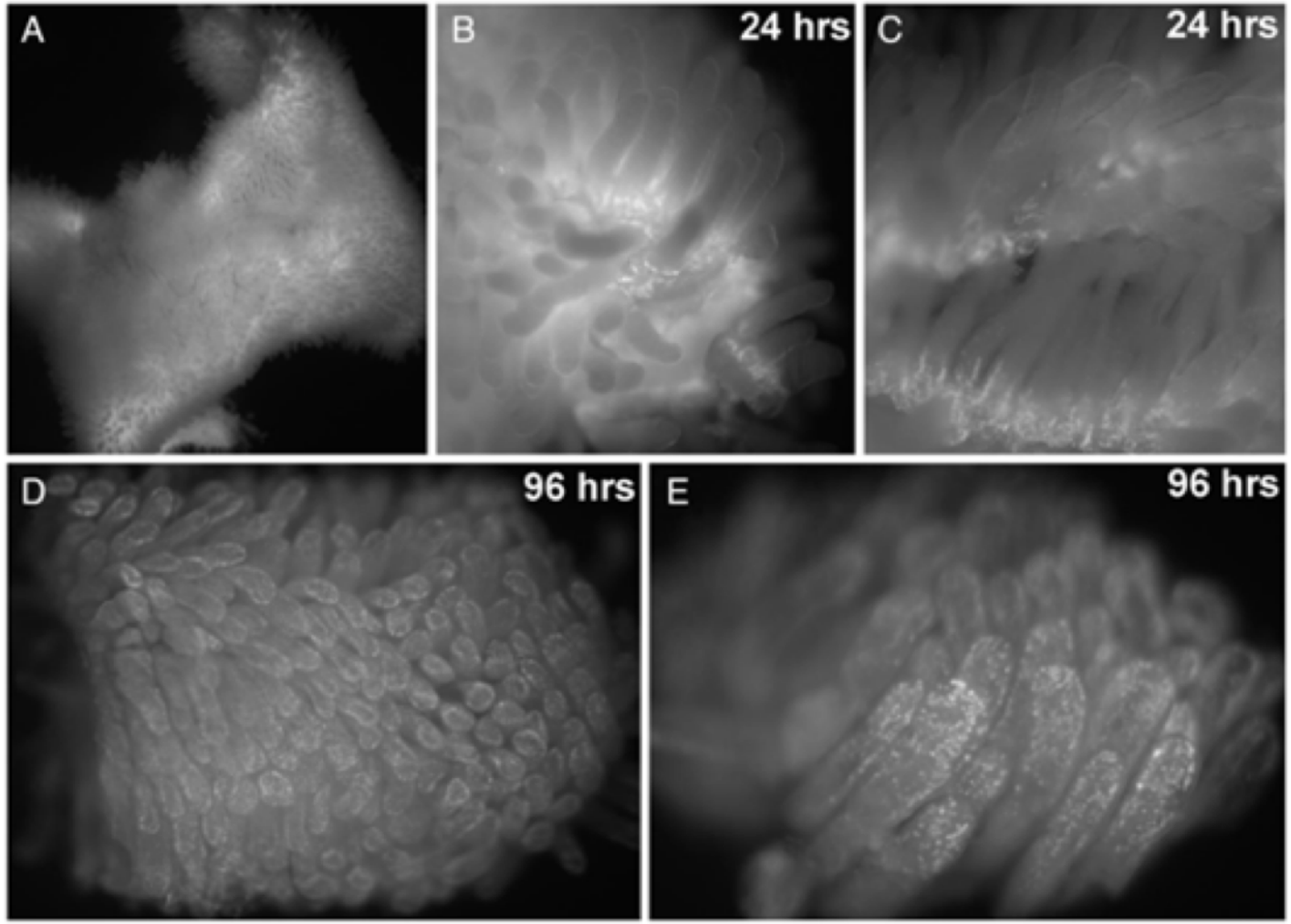

Fig. 5. Exploring cell proliferation and tissue dynamics in animals using EdU.

- Whole-mount fluorescent images of mouse small intestine, stained to detect EdU incorporation.

PNAS **2008**, *105*, 2415-20.

2. DNA labeling methods: b) Labeling newly synthesized DNA: EdU

Hoechst

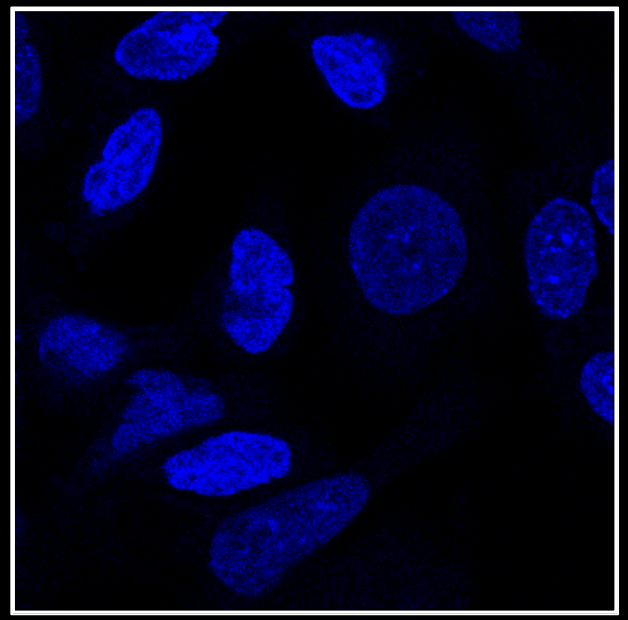

Alexa

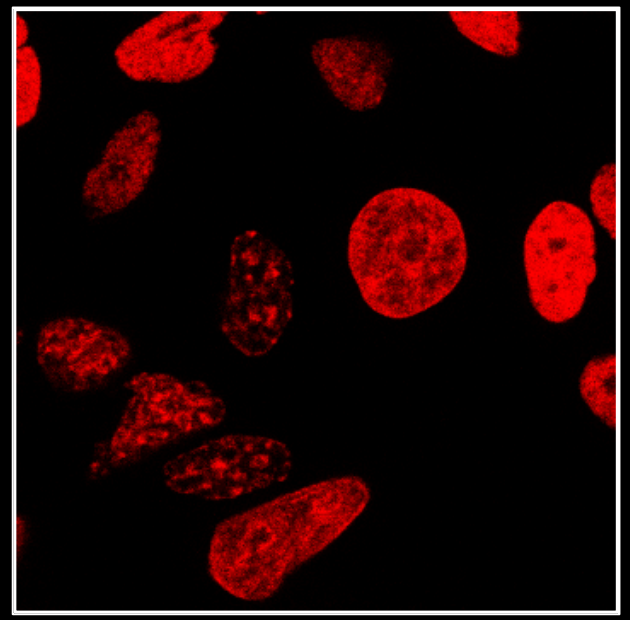

Overlay

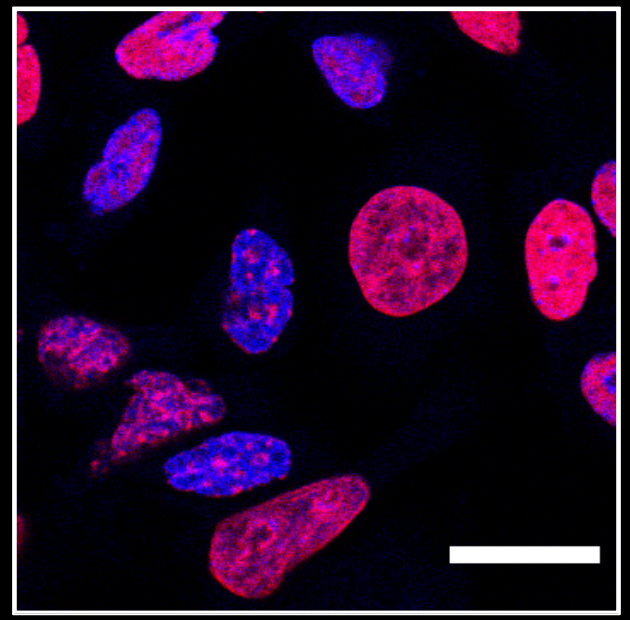

Confocal images of HeLa cells treated with EdU (10 µM, 16 h) before PFA fixation and labeling with Alexa647-azide and Hoechst33342, scale 25 µm.

2. DNA labeling methods: b) Labeling newly synthesized DNA: Unnatural pro-nucleotides

Pivaloyloxymethyl phosphotriester (=POM) is cleaved by endogenous esterases

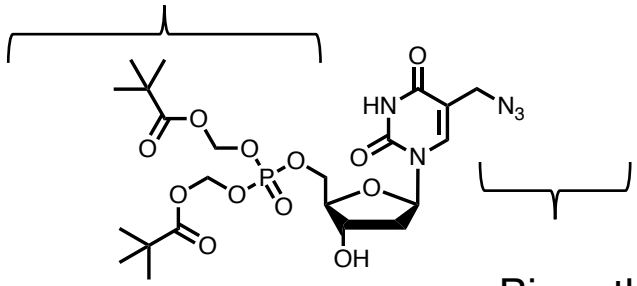

Bio-orthogonal handle for strain-promoted azide-alkyne cycloaddition (SPAAC)

$k \sim 0.01 – 1\ M^{-1}\ s^{-1}$

→ The larger the handle, the less likely to be a substrate of endogenous enzymes.

More efficient incorporation into DNA through protected monophosphate.

→ First phosphorylation is critical for incorporation into DNA.

Chembiochem **2018**, *19*, 1939-1943.

2. DNA labeling methods: c) CASFISH – a CRISPR-dCas9 method for fixed cells

- *In vitro* assembled dCas9/sgRNA fluorescently labels genomic DNA in cells
  - System is derived from Fluorescence-in situ hybridization (FISH), but no DNA denaturation needed.

    (i) CRISPR (clustered regularly interspaced short palindromic repeats) -dCas9 (nuclease-deficient caspase 9) mutant fused HaloTag labelled with JF646 (A)

    (ii) sgRNA that is targeting the desired sequences in the genome (B)

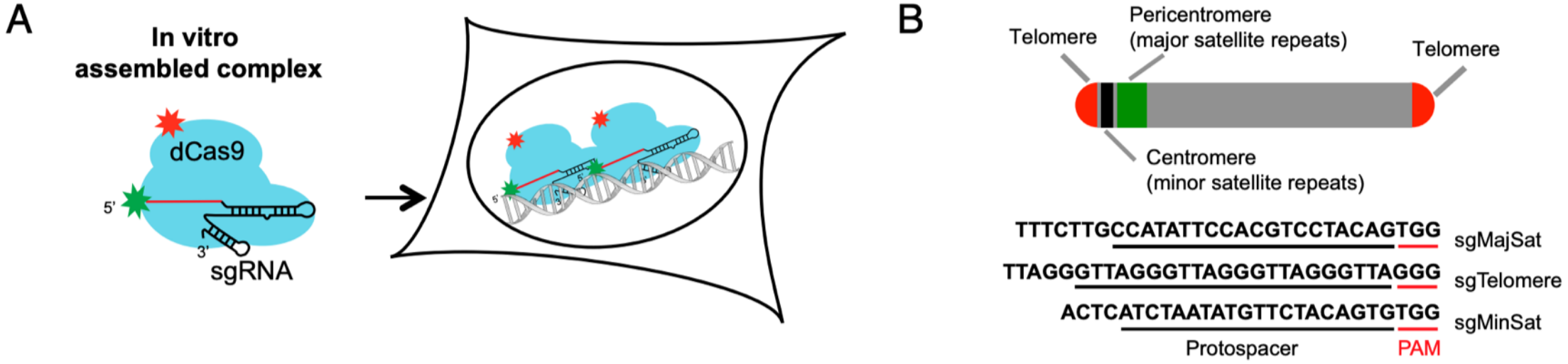

2. DNA labeling methods: c) CASFISH – a CRISPR-dCas9 method for fixed cells

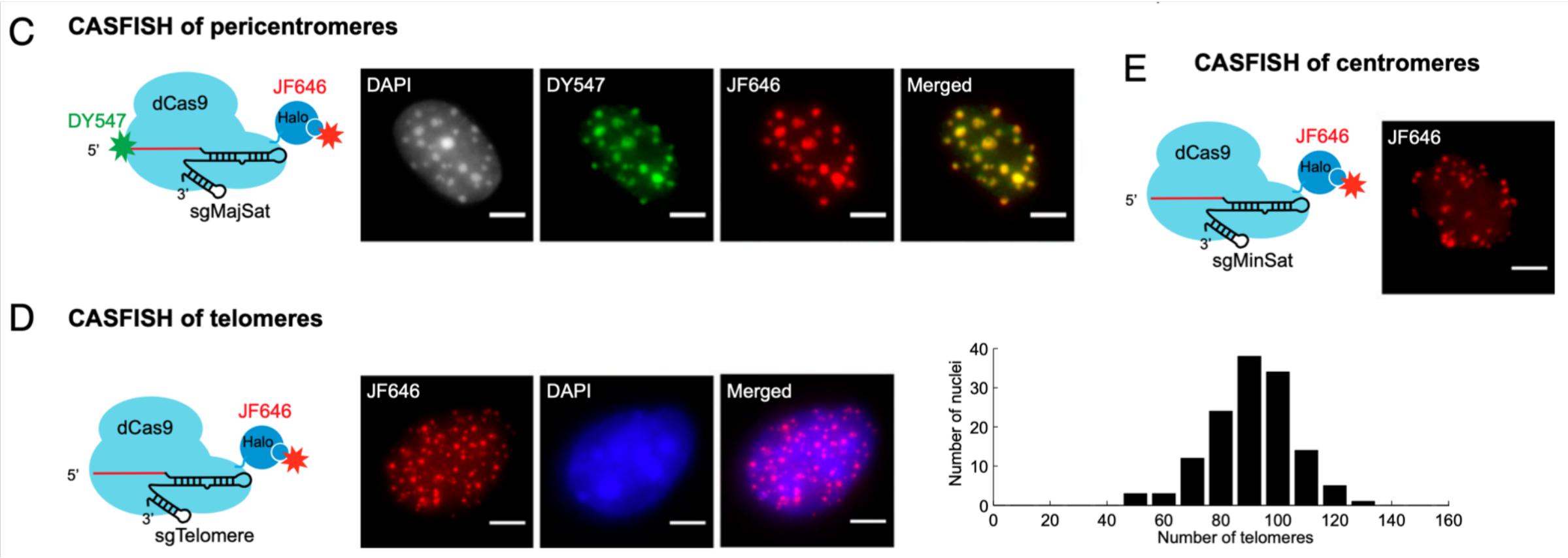

PNAS **2015**, *112*, *38*, 11870-1187.

MAX-PLANCK-GESELLSCHAFT

3. Paper: a) VdU: Rieder *et al.* - Alkene-Tetrazine Ligation for Imaging Cellular DNA

Angewandte
Communications

VIP DNA Labeling Very Important Paper

DOI: 10.1002/anie.201403580

Alkene–Tetrazine Ligation for Imaging Cellular DNA**

*Ulrike Rieder and Nathan W. Luedtke**

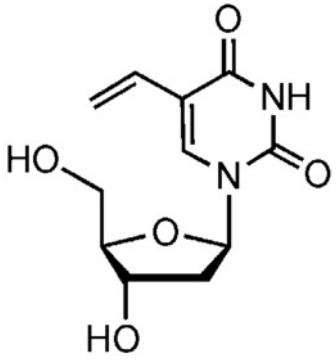

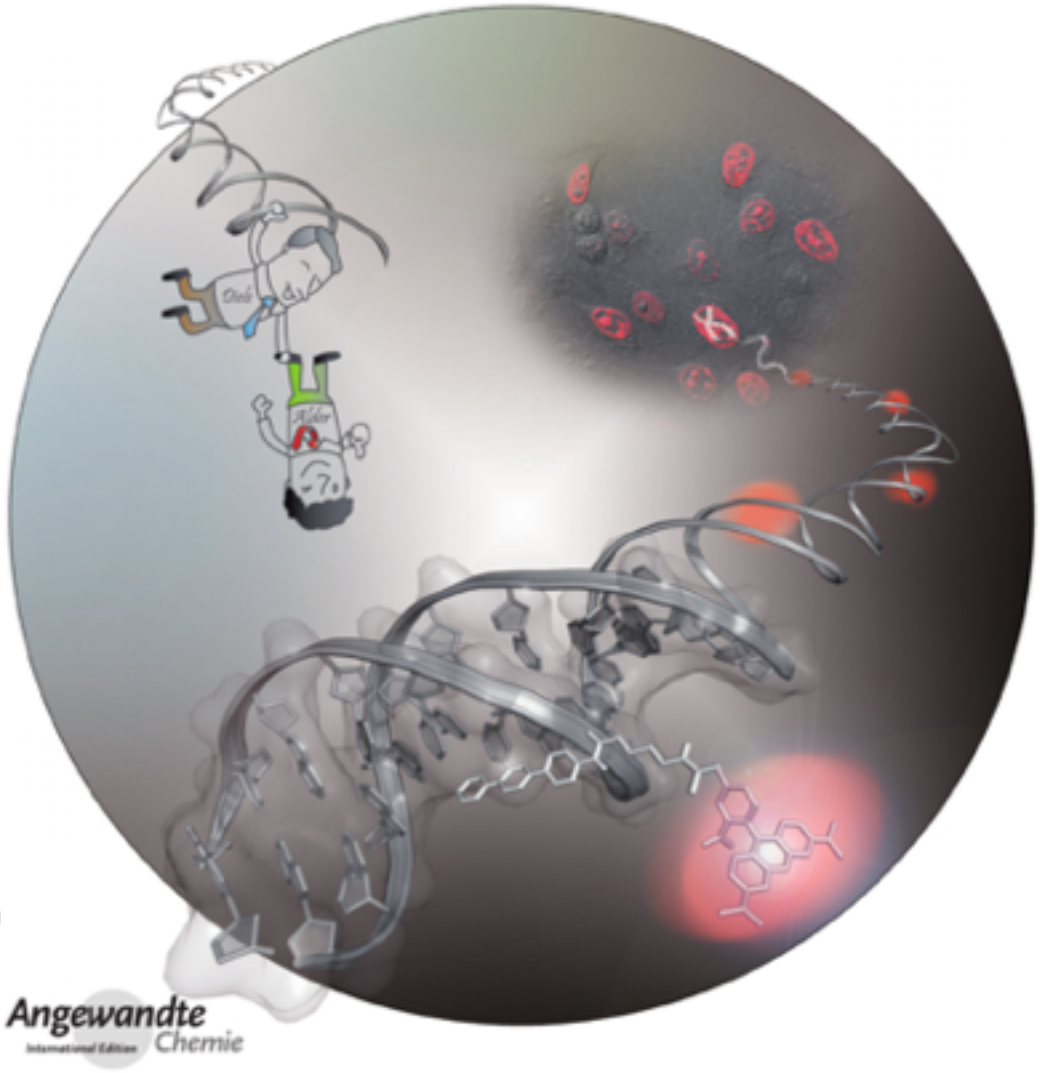

https://onlinelibrary.wiley.com/doi/epdf/10.1002/anie.201403580

3. Paper: a) VdU reacts with pyridyl-tetrazine but not EdU

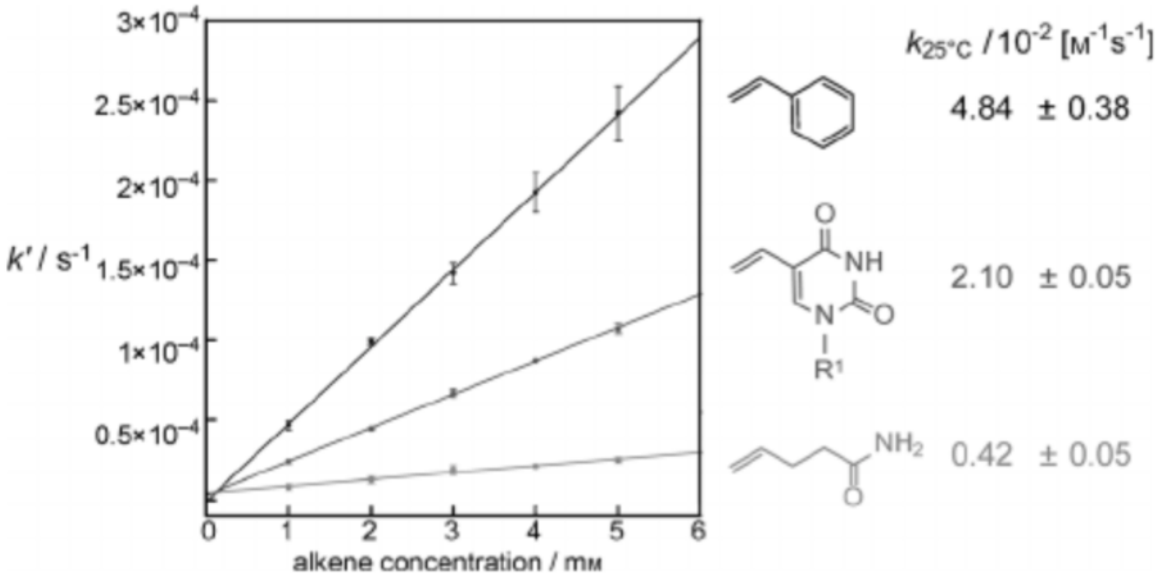

Figure 1. Pseudo-first-order reaction rates (k') versus alkene concentration for the consumption of tetrazine **5** (0.1 mM) in a 1:1 (v/v) mixture of methanol and water at 25 °C. The slope of each linear regression provides the rate constant k. R^1 = 2′-deoxyribose.

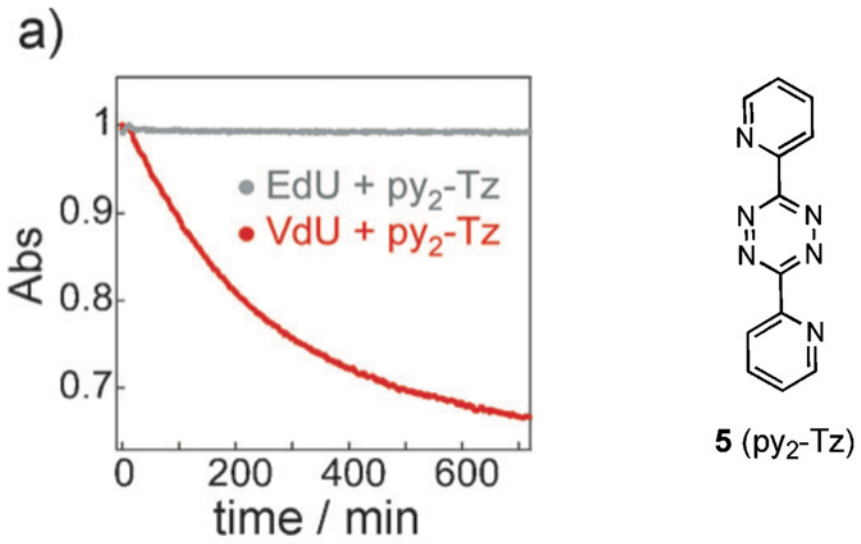

Figure 4. a) The consumption of tetrazine **5** (0.1 mM) according to normalized absorbance changes at 530 nm in the presence of 5 mM of EdU or VdU in a 1:1 (v/v) mixture of methanol and water at 25 °C.

→ The VdU ligation is bio-orthogonal to EdU.

3. Paper: a) VdU is incorporated into DNA and can be visualized with Tamra-Tz

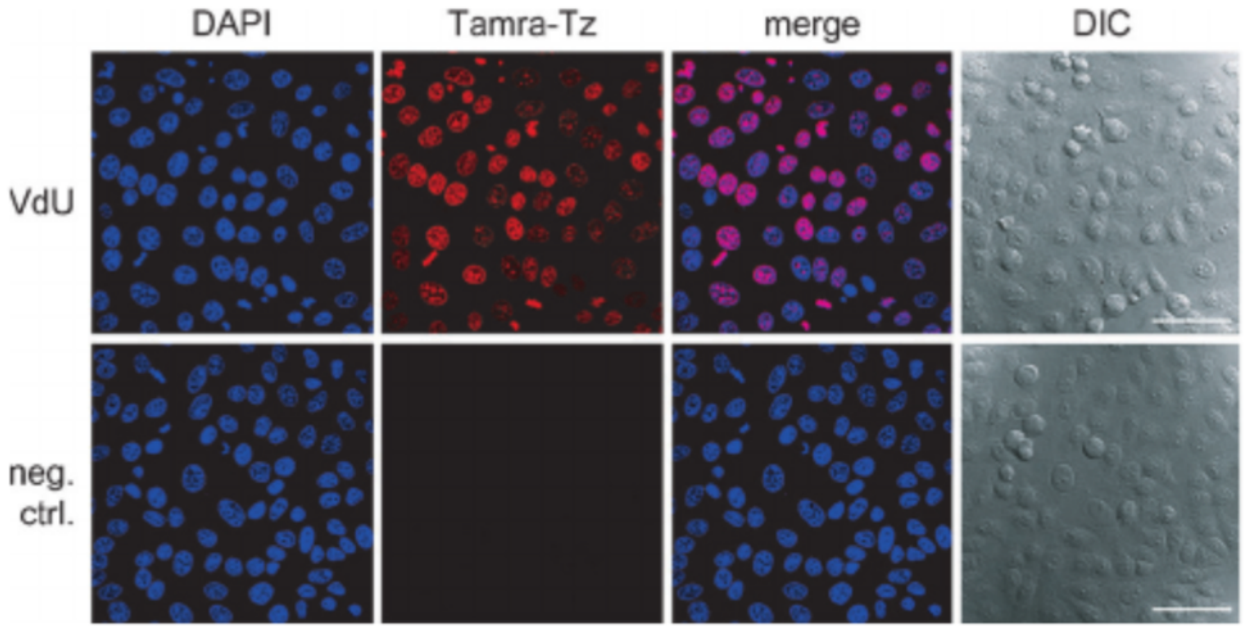

Figure 2. Bioorthogonal invDA ligation of VdU in newly synthesized DNA upon the addition of the fluorescent tetrazine Tamra-Tz. HeLa cells were treated with 30 μM VdU for 16 h, followed by fixation, DNA denaturation, and incubation with 5 μM Tamra-Tz for 4 h. Total cellular DNA was stained with DAPI. The negative control (neg. ctrl.) samples received identical treatment but were not incubated with VdU prior to staining. Scale bars: 50 μm. DIC = differential interference contrast image, merge = overlay of Tamra-Tz and DAPI channels.

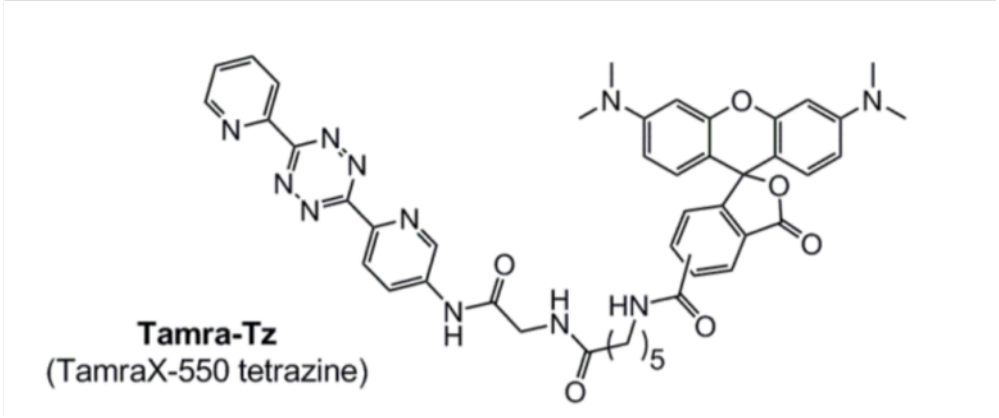

3. Paper: a) VdU is less toxic than EdU

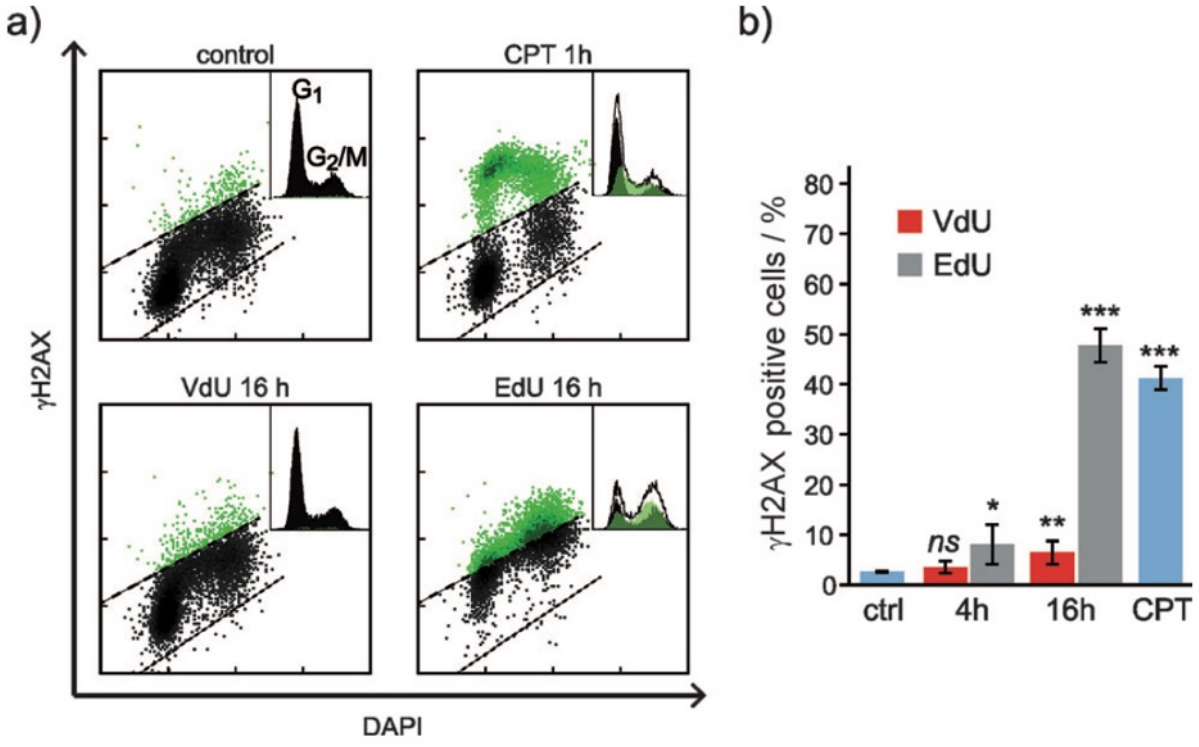

Figure 3. Flow cytometry analysis of γH2AX versus DAPI staining of HeLa cells treated with 30 μM VdU or 10 μM EdU for 16 h. These concentrations were selected based upon the equivalent staining frequencies and intensities observed for EdU and VdU (Figure 4 b, c, and Figure S15, 16). γH2AX positive cells were detected by using a phosphospecific antibody. a) The dot plots illustrate γH2AX abundance versus the total cellular DNA content of each cell. The insets display histograms of the DNA content (from the cell cycle phases $G_0/_1$ to G_2/M) versus cell count. The dashed lines show the thresholds used for defining γH2AX positive/negative cells based on the control. For a positive control, cells were treated for 1 h with camptothecin (CPT, 0.5 μM), which causes DNA damage.[21] b) A graphical representation of results where $n = 5$, $*P < 0.02$, $**P < 0.002$, $***P < 0.0001$, ns = not significant, compared to the control. For 4 h time points and U2OS cells see Figure S11.

→ VdU less toxic as phosphorylation of histones H2AX is less pronounced.

→ γH2AX formation is associated with DNA strand breakage.

3. Paper: a) VdU can be used for multicolor imaging of newly synthesized DNA

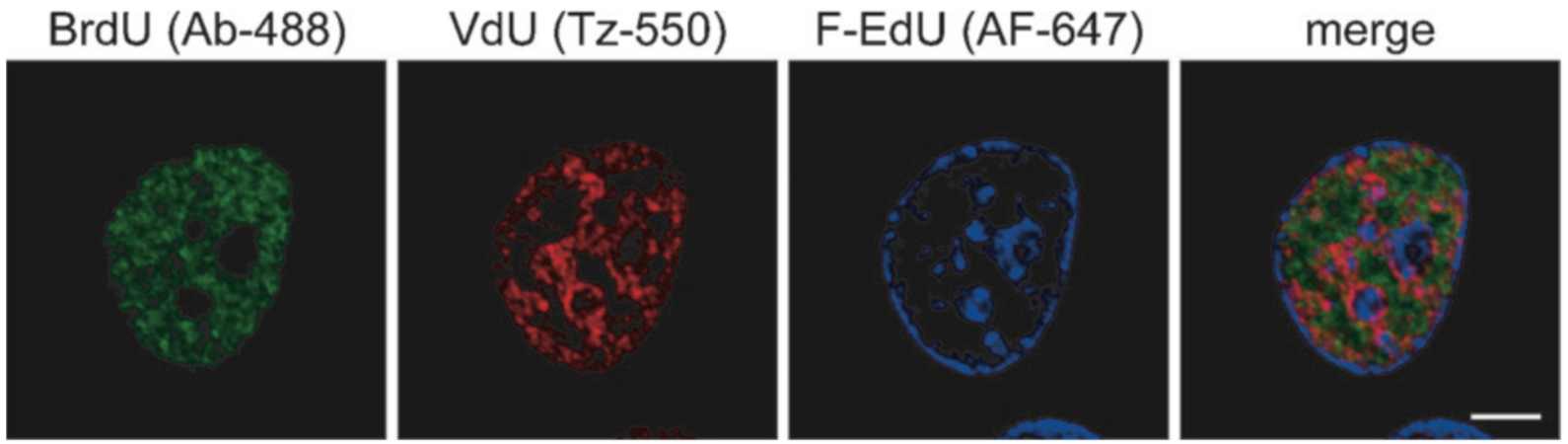

Figure 5. Visualizing the progression of the S-phase in a single cell by using BrdU (30 µM, 1st pulse, green), VdU (30 µM, 2nd pulse, red), and F-*ara*-EdU (10 µM, 3rd pulse, blue). HeLa cells were incubated for 2 h 45 min with each nucleoside and washed for 15 min with fresh media in between nucleoside treatments. After fixation and DNA denaturation, the cells were stained with Tamra-Tz (red), BrdU antibody (green), and AF-azide (blue). Scale bars: 5 µm. See Figure S17 for additional examples.

Cell cycle: